

1 ***Flying too close to the Sun – the viability of perihelion-induced aqueous alteration on***
2 ***periodic comets***

3 Suttle, M.D.^{1,2,*} (corresponding author), Folco, L^{2,3}, Genge, M.J.^{2,4} Russell, S.S.,²
4 martindavid.suttle@dst.unipi.it, luigi.folco@unipi.it, m.genge@ic.ac.uk, sara.russell@nhm.ac.uk

5
6 ¹Planetary Materials Group, Department of Earth Sciences, Natural History Museum, Cromwell
7 Road, London, SW7 5BD, UK

8 ² Dipartimento di Scienze della Terra, Università di Pisa, 56126 Pisa, Italy

9 ³CISUP, Centro per l'Integrazione della Strumentazione dell'Università di Pisa, Lungarno Pacinotti 43,
10 56126 Pisa, Italy

11 ⁴Impacts and Astromaterials Research Centre, Department of Earth Science and Engineering,
12 Imperial College London, South Kensington, London, SW7 2AZ, UK

13
14 **Abstract**

15 Comets are typically considered to be pristine remnants of the early solar system. However, by
16 definition they evolve significantly over their lifetimes through evaporation, sublimation, degassing
17 and dust release. This occurs once they enter the inner solar system and are heated by the Sun. Some
18 comets (e.g. 1P/Halley, 9P/Tempel and Hale-Bopp) as well as chondritic porous cosmic dust – released
19 from comets – show evidence of minor aqueous alteration resulting in the formation of phyllosilicates,
20 carbonates or other secondary phases (e.g. Cu-sulphides, amphibole and magnetite). These
21 observations suggest that (at least some) comets experienced limited interaction with liquid water
22 under conditions distinct from the alteration histories of hydrated chondritic asteroids (e.g. the CM
23 and CR chondrites).

24 This synthesis paper explores the viability of perihelion-induced heating as a mechanism for the
25 generation of highly localised subsurface liquid water and thus mild aqueous alteration in periodic
26 comets. We draw constraints from experimental laboratory studies, numerical modelling, spacecraft
27 observations and microanalysis studies of cometary micrometeorites. Both temperature and pressure
28 conditions necessary for the generation and short-term (hour-long) survival of liquid water are
29 plausible within the immediate subsurface (<0.5m depth) of periodic comets with small perihelia (<1.5
30 A.U.), low surface permeabilities and favourable rotational states (e.g. high obliquities and/or slow
31 rotational periods). We estimate that solar radiant heating may generate liquid water and perform
32 aqueous alteration reactions in 3-9% of periodic comets. An example of an ideal candidate is 2P/Encke
33 which has a small perihelion (0.33 A.U.), a high obliquity and a short orbital period. This comet should
34 therefore be considered a high priority candidate in future spectroscopic studies of comet surfaces.
35 Small quantities of phyllosilicate generated by aqueous alteration may be important in cementing
36 together grains in the subsurface of older dormant comets, thereby explaining observations of
37 unexpectedly high tensile strength in some bodies.

38 Most periodic comets which currently pass close to the Sun are dormant, having experienced surface
39 heating, significant cometary activity and dust release in the past. These bodies may be responsible
40 for the partially hydrated cometary micrometeorites we find at the Earth's surface and their aqueous
41 alteration histories may have been produced by perihelion-induced subsurface heating. This is in
42 contrast to radiogenic and impact heating that operated during the early solar system on asteroids.
43 This study has implications for the alteration history of the active asteroid Phaethon, the target of
44 JAXA's DESTINY+ mission.

48 **1. Introduction – laboratory perspective on naturally delivered cometary dust**

49 Chondritic porous (CP) cosmic dust (micrometeorites and interplanetary dust particles [IDPs]) are
50 nominally anhydrous, poorly crystalline silica-rich carbonaceous and porous aggregates composed of
51 nano- to micron-sized grains (Mackinnon and Rietmeijer, 1987; Noguchi et al., 2015; 2017). Their
52 primary components are amorphous GEMS (glass with embedded metal and sulphides [Bradley, 1994;
53 2019]), which represent either moderately volatile, late-stage nebula condensation products, formed
54 at temperatures <750°C (Keller and Messenger, 2011) or interstellar relict grains, recording formation
55 environments prior to the birth of the solar system at temperatures <200°C (Ishii et al., 2018).
56 Chondritic porous dust also contains crystalline anhydrous silicates, which can vary significantly in
57 solid solution composition within a single particle, spanning the entire range of silicates found within
58 chondrites (Klöck et al., 1989; Flynn, 1994; Noguchi et al., 2017). In addition, more exotic highly
59 refractory Mg-enriched silicates are known, which are otherwise rare or absent among meteorites.
60 They include LIME (low iron Mn-enriched) and LICE (low iron Cr-enriched) silicates (Klöck et al., 1989),
61 kosmochloric (Na-Cr-rich) pyroxenes (*kool grains*, Joswiak et al., 2009) and condensation-crystallized
62 enstatite whiskers (Stodolna et al., 2014). Consequently, the anhydrous silicates within CP-dust are
63 fragments of primitive, high-temperature materials, several of which are associated with
64 condensation crystallization and potentially related to the first-generation chondrules and CAIs.

65 Chondritic porous dust is closely related to ultracarbonaceous micrometeorites, which contain higher
66 abundances of carbonaceous matter (>50wt.%, Dobrică et al., 2009; Duprat et al., 2010) but are
67 otherwise petrographically similar. Together these two subclasses are widely accepted as cometary in
68 origin, owing to their exotic mineralogies, volatile-rich bulk compositions, unique isotopic signatures
69 – which may show extreme isotopic excursions and distinctive “*bunch-of-grapes*” morphologies
70 (Duprat et al., 2010; Starkey et al., 2014; Noguchi et al., 2015). Likewise, they share many similarities
71 to the known cometary dust recovered from the short-period comet 81P/WILD 2 (Zolensky et al.,
72 2006; 2008; Dobrică et al., 2009). Thus, cometary materials contain high-temperature early-formed
73 refractory silicates intimately mixed with amorphous volatile matrix (GEMS, Fe-oxides and Fe-sulfides)
74 and super-volatiles (carbonaceous matter and ices).

75 **2. Evidence for early stage aqueous alteration in cometary dust**

76 Like all chondritic materials, cometary dust particles preserve a record of its parent body’s geological
77 activity. For many of the naturally delivered cometary dust particles evidence for minor or “*early*
78 *stage*” aqueous alteration has been reported. Several studies describe various stages of hydration and
79 secondary replacement in cometary dust aggregates. This ranges from the leaching of Mg and S and
80 the partial hydration of GEMS (Nakamura et al., 2005; Noguchi et al., 2017; Yabuta et al., 2017)
81 through to their complete conversion to low-crystallinity Fe-rich phyllosilicates and the development
82 of complex multi-species phyllosilicate intergrowths with well-defined lattice parameters (Rietmeijer,
83 1991). Furthermore, Busemann et al. (2009) identified both carbonates and amphibole (anthophyllite
84 [Mg₂Mg₅Si₈O₂₂(OH)₂], occurring in association with GEMS) within a single micrometeorite. This particle
85 purportedly originates from the Pi-Puppis meteor stream (and consequently from the Jupiter family
86 comet [JFC] 26P/Grigg–Skjellerup [Vaubaillon and Colas, 2005]). Both minerals are widely associated
87 with secondary alteration phases in carbonaceous chondrite settings. Amphiboles in particular were
88 a highly unusual discovery, having a hydrated composition (containing structural water) and
89 associated with hydrothermal activity (Dobrică and Brearley, 2014). These phases may represent
90 either alteration minerals or primary condensation phases (although the latter interpretation is

91 favoured by [Busemann et al., 2009](#)). In most instances, aqueous alteration extent in cometary dust is
92 minor, restricted to the hydration of GEMS and their subsequent conversion to Fe-rich proto-
93 phyllosilicates, without the concurrent alteration of mafic silicates (olivine and pyroxene) ([Nakamura-
94 Messenger et al., 2011](#)).

95 Likewise, intense study of the 81P/Wild cometary grains captured and returned by the STARDUST
96 mission has also identified tentative evidence of aqueous alteration. This includes the presence of
97 possible secondary minerals: carbonates ([Flynn et al., 2008; 2009](#)), (Ti-free) magnetite (formed by
98 oxidation at temperatures <300°C, [Hicks et al., 2017](#)) and Cu-, Zn- and Fe- sulphides ([Berger et al.,
99 2011; 2015](#)). Cubanite in particular provides constraints on the comet's alteration environment,
100 limiting conditions between 150-200°C, with alkaline fluids (pH~9) and oxygen fugacities at the iron-
101 wüstite buffer ([Berger et al., 2015](#)). However, to date, phyllosilicates have not been observed in
102 laboratory analyses of this comet's mineral assemblage returned by the STARDUST mission ([Zolensky
103 et al., 2006; 2008](#)). This is despite the expected survival of phyllosilicate or their decomposition phases
104 within the aerogel capture medium ([Noguchi et al., 2007; Zolensky et al., 2008; Wozniakiewicz et al.,
105 2010](#)).

106 **3. Experimental studies constraining the duration of aqueous alteration**

107 Nelson et al., ([1987](#)) performed early pioneering aqueous alteration experiments on cometary
108 analogue materials. They used synthetic amorphous magnesio-silica smokes with simple compositions
109 (Mg-SiO) and amorphous structures as approximations of natural cometary dust. These amorphous
110 silicates were reacted with distilled water at several different temperatures (58°C, 83°C, 95°C and
111 105°C) under atmospheric pressures (~101kPa) and for durations between 1 and 142 hours resulting
112 in the formation of sepiolite ($\text{Mg}_4\text{Si}_6\text{O}_{15}(\text{OH})_2 \cdot 6\text{H}_2\text{O}$) – a complex phyllosilicate of the palygorskite-
113 sepiolite group. After terminating each reaction, IR spectroscopy was used to measure the degree of
114 alteration using peak intensity ratios at three key wavelengths, which reflect the decay (11.5µm) of
115 the initial amorphous structure and growth (16µm and 20µm) of hydrated phases. The primary aim
116 was to investigate the kinetics of hydration reactions under conditions relevant to asteroids and
117 comets. This study concluded that reactions occur rapidly (over hours to days) and that reaction rates
118 follow a power law function with a strong temperature dependence (Fig.1). Consequently, over the
119 temperature range (-25°C to +25 °C) reaction rates increase five-fold for every +10°C temperature
120 increase. This translates to reaction half-lives of approximately 80 hours at 80°C, 300 hours at 50°C
121 and 2000 hours at 20°C (Fig.1).

122 The reactions of Nelson et al., ([1987](#)) provide important constraints on the kinetics of hydrated
123 amorphous silicates. However, their experimental products (sepiolite) are more complex partial chain
124 silicates with higher water content than the Fe-rich saponite and serpentines observed in hydrated
125 cometary dust ([Noguchi et al., 2017; Yabuta et al., 2017](#)). Thus, although the kinetic temperature
126 dependence relationship measured by Nelson et al., ([1987](#)) is likely to be accurate in the general sense
127 (applicable to the hydration of amorphous silicates), the reaction rates and therefore the reaction
128 durations are significant overestimates, since the formation of simpler, less hydrated phyllosilicates
129 requires shorter timescales and possibly lower activation energies. Differences in reaction products
130 between the experiments of Nelson et al., ([1987](#)) and the naturally altered materials most likely
131 originate from two sources:

132 (1) Different starting compositions affect reactions trajectories. Naturally occurring GEMS have
133 stoichiometries of approximately $(\text{Mg,Fe})\text{SiO}_3$ ([Keller and Messenger, 2011](#)) and thus contain
134 significant Fe^{2+} . In addition, GEMS have embedded metal and sulphide phases with measured bulk S
135 contents at ~2-5 Atomic% ([Bradley, 1994](#)). The presence of Fe and S is critical in determining how
136 GEMS alter. This is because first-formed phyllosilicates in cometary dust and chondritic matrix are
137 almost always Fe-rich endmembers, while the Mg in GEMS appears to be more fluid-mobile, being

138 carried away in the alteration fluid and employed in distal alteration reactions (Leroux et al., 2015;
139 Noguchi et al., 2017).

140 (2) Additionally, Nelson et al., (1987) used the appearance of 16 μ m and 20 μ m peaks in the IR spectrum
141 of their alteration products to confirm the generation of phyllosilicates. However, the IR spectral
142 features of poorly crystalline hydrated silicates will be weak broad and smooth signals and are
143 therefore not easily detected by IR methods. Thus, in the experiments of Nelson et al., (1987) their
144 phyllosilicate detection method is likely to have missed subtle proto-phyllosilicates and instead only
145 registered the formation of well-developed crystalline forms. In this case, the calculated reaction
146 times will be overestimates of the true reaction times needed to form more primitive poorly-
147 crystalline species.

148 Rietmeijer et al., (2004) built on the experimental design on Nelson et al., (1987), also using
149 amorphous magnesio-silica smokes and investigating reaction products with both IR and TEM
150 (transmission electron microscopy). They similarly concluded that characterisation by IR techniques
151 alone is inconclusive because “fluffy” phyllosilicate forms remain unidentified and that reaction rates
152 determined for the development of sepiolite do not accurately model cometary alteration which
153 produces simpler phyllosilicates. In this study they conclude that sample permeability plays a
154 fundamental role in the rate of alteration. As alteration proceeds porosity decreases dramatically
155 because low-density amorphous structures collapse while hydrated phyllosilicates swell. This
156 behaviour means that further alteration beyond an initial poorly crystalline phase is limited as porosity
157 becomes the rate limiting step.

158 Later Nakamura-Messenger et al., (2011) performed aqueous alteration experiments using pre-
159 characterised anhydrous CP-IDPs as the starting material. They exposed these natural samples to
160 neutral and alkaline water (pH 7-13) at temperatures between 25°C and 160°C for durations between
161 12-48 hrs. These experiments demonstrated that GEMS can alter to Fe-rich phyllosilicates (both
162 serpentine and saponite species) at low temperatures (25°C) in alkaline solutions (pH 12-13) within
163 less than 12 hours. This study therefore confirms that reaction rates for the hydration of amorphous
164 silicate are at least two orders of magnitude faster than previously predicted by Nelson et al., (1987)
165 and displayed here in Fig.1.

166 More recent experiments by Takigawa et al., (2019) exposed amorphous silicate analogues to water
167 vapour (explicitly not liquid water) at low temperatures (-30°C to +50°C) over long durations (10-120
168 days) but found that alteration reactions cannot occur unless vapour temperatures are sustained
169 above 0°C (25°C being their first above-zero run temperature in which alteration was observed).
170 Abundant observations of comets have confirmed the presence of outgassing water vapour within
171 cometary comae (e.g. Weaver et al., 1988; Russo et al., 2000; Feaga et al., 2007; Bockelée-Morvan et
172 al., 2015). Therefore, primitive amorphous cometary silicates will be exposed to water vapour during
173 perihelion passage. This likely forms a thin aqueous layer on silicate surfaces – which if heated
174 sufficiently – could lead to surface aqueous alteration reactions (as demonstrated experimentally by
175 Takigawa et al., 2019). Water vapour has a much longer orbital window than liquid water (generally
176 forming once comets are within 3 A.U. of the Sun [Biver et al., 1997]) and thereby ensuring sustained
177 interaction. However, vapour-facilitated alteration reaction rates are likely to be significantly slower
178 than those caused by liquid water interaction, as demonstrated by comparing the <24hr liquid water
179 alteration timescales seen by Nakamura et al. (2011) against the 100-1000hr vapour phase alteration
180 timescales of Takigawa et al. (2019). Furthermore, because aqueously altered cometary dust is
181 relatively rare, while vapour-silicate interaction should be ubiquitous, it is unlikely that vapour
182 reactions play a critical role in the aqueous alteration of cometary materials. Instead, the limited
183 evidence of aqueously alteration on only a small number of comets is best explained if liquid water is
184 required before hydration reactions occur. A detailed investigation of vapour phase silicate interaction
185 extends beyond the scope of this paper but requires future research attention.

186 4. Possible energy sources for the aqueous alteration on comets

187 The two leading hypotheses for the source of heat energy driving aqueous alteration (and thermal
188 metamorphism) on hydrated chondritic asteroids are (1) planetesimal-scale high-energy impact
189 events (Rubin, 2012; Lindgren et al., 2015; Vacher et al., 2018) and (2) the radioactive decay of short-
190 lived isotopes (e.g. ^{26}Al , Keil 2000; McSween et al., 2002). Both mechanisms provide sufficiently high
191 temperatures and sufficiently long durations, as defined by experimental and petrographic constraints
192 from meteorite studies and are, therefore, consistent with the expected alteration environments of
193 asteroids. For example, the alteration of CM chondrites appears to have reached temperatures as high
194 as 300°C. These estimates are based on the O-isotopic fractionation signatures preserved in secondary
195 phases, primarily carbonates (Guo and Eiler, 2007 [20-71°C]; Verdier-Paoletti et al., 2017 [50-300°C];
196 Vacher et al., 2019 [-10 to 250°C]). Aqueous alteration in CM chondrites occurred over exceptionally
197 long durations, perhaps several millions of years (as inferred from ^{53}Mn - ^{53}Cr dating by Lee et al.,
198 [2012]). However, the growth of individual crystals is likely to have been episodic in nature (de Leuw
199 et al., 2009; Lee et al., 2012). Thus an impact heating scenario (for the CMs [at least]) is also capable
200 of explaining the O-isotopic fractionation signatures, the weak correlation observed between the
201 degree of aqueous alteration, and the strength of petrofabrics as well as the prevalence of crushed
202 chondrules (Rubin, 2012; Hanna et al., 2015; Lindgren et al., 2015; Vacher et al., 2018).

203 In contrast to the thermal histories of asteroids, both radiogenic and impact heating may have been
204 inefficient or entirely absent as heating mechanisms for cometary parent bodies originating in the cold
205 outer solar system. This is because the parent bodies of comets are generally assumed to have formed
206 in a low-density region of the early solar system, resulting in significantly fewer collisions and thus a
207 greatly reduced impact energy for internal heating (Davidsson et al., 2016). Furthermore, cometary
208 parent bodies are likely to have formed later than asteroids. This delayed growth would avoid
209 appreciable thermal processing generated by the radiogenic decay of short-lived isotopes, primarily
210 ^{26}Al whose half-life is just 0.73Ma (Podolak and Prialnik, 1997; Mousis et al., 2017). Choi et al., (2002)
211 estimated that Kuiper Belt objects would have, in the best-case scenarios, achieved temperatures only
212 as high as -93°C as a result of ^{26}Al decay. Additionally, this heating would be localised to the parent
213 body's core, while the outer layers would have remained unheated. Similarly, Prialnik et al., (1987)
214 argued that observations of outgassing at surprisingly large heliocentric distances (5.8-11.4 A.U.)
215 which are currently attributed to the annealing of amorphous ice when comets first enter the inner
216 solar system (Prialnik and Bar-Nun, 1990; 1992; Meech et al., 2009) – provides a clear constraint on
217 the maximum parent body temperatures ($T < -138^\circ\text{C}$) experienced by cometary parent bodies over
218 their lifetimes.

219 Recent suggestions have, however, challenged this argument. There is growing recognition that
220 asteroids and comets potentially form a continuum of objects with transitional properties (Hartmann
221 et al., 1987; Gounelle, 2011; Nuth et al., 2019). Notably, some cometary parent bodies may in fact
222 have originated in the inner solar system and experienced asteroidal processing (e.g. CM-like
223 alteration induced by radiogenic or impact mechanisms). These bodies were later ejected outwards
224 during the giant planet migration phase (Walsh et al., 2012). They would then have developed further
225 during a second phase of volatile accretion, covering their asteroidal interior with a cometary cover
226 (Meech et al., 2016; Nuth et al., 2019). Such bodies are termed Manx comets (named after a cat breed
227 that lack tails) and are nearly inactive, either lacking a characteristic cometary tail or having a weak
228 tail owing to their thin volatile covers (Meech et al., 2016)¹. In these bodies phyllosilicates would be

¹ In the future, the classification of small bodies as either hydrous/ice-bearing or anhydrous may therefore serve as more meaningful grouping than asteroid and comet.

229 explainable simply as a product of their warm early alteration before subsequent residence in the
230 outer solar system. However, Manx comets are expected to be relatively rare components of the solar
231 system and not the most common type of comet. For example, among the 106 long-period comets
232 studied by Meech et al., (2016) just 2 were found to have minimal activity and thus be potential Manx
233 comets (Engelhardt et al., 2017).

234 Conversely, if both impact and radiogenic heating were indeed inactive on most cometary parent
235 bodies, then an alternative model is required to explain the mild aqueous alteration activity expected
236 in (some) comets (Noguchi et al., 2017). For example, aqueous alteration may have been a late-stage
237 feature, occurring only once a comet enters the inner solar system and where perihelion heating by
238 the Sun was able to warm the subsurface layers allowing liquid water to temporarily exist immediately
239 prior to degassing and coma formation. Such a scenario would also be consistent with the preservation
240 of amorphous ice until solar heating causes recrystallization and/or sublimation.

241 **5. Can Perihelion heating generate subsurface liquid water?**

242 To explore whether liquid water is viable requires consideration of the subsurface conditions inside
243 comets as they approach perihelion. Solar radiant heating would need to generate sufficient
244 subsurface pressure and temperature regimes over timescales on the order of hours, at least, if
245 reactions with silicates are to occur. This short-term survival will be dependent on two factors (1)
246 temperature and (2) pressure, as shown by the phase diagram of water, with the stability field of liquid
247 water highlighted (Fig.2). For pure liquid water to be present the pressure and temperature at the
248 triple point must be exceeded ($T > 0.01^\circ\text{C}$ and $P > 611.2\text{ Pa}$). We consider each variable in turn:

249

250 **(1) Temperature:** Surface temperatures for several comets over a range of heliocentric distances have
251 now been measured by spacecraft using thermal infrared techniques. These include 1P/Halley by the
252 Soviet space probe Vega-1 (Emerich, et al., 1986), 19/P Borrelly by NASA's Deep Space 1 mission
253 (Soderblom et al., 2004), 9P/Tempel (Tempel 1) and 103P/Hartley by the NASA's Deep Impact mission
254 (Groussin et al., 2013) and most recently, 67P/Churyumov–Gerasimenko by ESA's Rosetta mission
255 (Tosi et al., 2019) (Fig.3). These empirical measurements, collectively define a power-law relationship
256 between surface temperature and heliocentric distance (Fig.3) and demonstrate that surface
257 temperatures between $0\text{--}120^\circ\text{C}$ may be reasonably inferred for comets with perihelion distances
258 $< 1.5\text{A.U.}$ The next logical question to consider therefore is how surface temperatures are related to
259 subsurface temperatures?

260 Thermal conduction is the primary mechanism by which surface heat will migrate inwards through the
261 comet's subsurface (although other processes such as gas-driven convection and radiative heat
262 transfer may also be important, these are considered in detail below). Thermal conduction within
263 comets is highly inefficient due to the presence of porous amorphous ice (Kouchi et al., 1992).
264 Conduction is further inhibited by the presence of non-volatile dust-rich crusts that develop on comets
265 as they survive multiple perihelion passes (Kömlé and Steiner, 1992; Schulz et al., 2015; Quirico et al.,
266 2015; Miles, 2016). Thus, comets have low thermal inertia, with quoted values typically given at
267 $< 50\text{WK}^{-1}\text{m}^{-2}\text{s}^{1/2}$ (Fernandez et al. 2002; Lisse et al. 2005; Groussin et al., 2007; 2013; Davidsson et al.,
268 2013; Shi et al., 2016) consistent with the measured thermal inertia for 67P ($85 \pm 35\text{WK}^{-1}\text{m}^{-2}\text{s}^{1/2}$, Spohn
269 et al., 2015). In consideration of these factors Wickramasinghe et al., (2009) also explored the
270 possibility of perihelion-induced liquid water, using numerical modelling to estimate internal
271 subsurface temperatures, based on a three-layer model (top: "burnt asphalt", middle: porous organic-
272 rich crust and base: water-ice layer). This study concluded that solar radiant heating can penetrate to
273 depths on the order of 1m. In their model, the overall relationship between surface and subsurface
274 temperatures is described by an exponential relationship:

275 $T_Z = Se^{(-AZ)}$ (eq. 1)

276 Where:

277 T_Z = internal temperature T at depth Z.

278 S = Surface temperature

279 A = the slope function (a constant), varying between 0.006 and 0.008 (here we use the avg. value of
280 0.007).

281 Z = depth within the comet (given in cm).

282 Using this model equation, we input the average temperature data from the five periodic comets with
283 measured surface temperatures (1P, 9P, 19P, 67P and 103P), thereby allowing an approximation of
284 their subsurface temperature profiles during perihelion (Fig.4). The model of Wickramasinghe et al.,
285 (2009) therefore suggests that temperatures >0°C may be attainable for subsurface depths <40cm in
286 bodies with perihelia <1.5.A.U.

287 Alternative studies provide additional estimates on the heat transfer dynamics through a cometary
288 subsurface. For example, direct observations of the comet 9P/Tempel allowed the production of a
289 surface temperature map (generated prior to impact). This indicated that the penetration of surface
290 heat is likely to be highly limited (Groussin et al., 2007), perhaps on scales of <10cm and thus less
291 pronounced than in the model of Wickramasinghe et al., (2009). Similarly, empirical observations
292 during the approach to 9P/Tempel Deep Impact noted the release of volatile H₂O (and CO₂) during
293 early plume activity which appeared to originate from the immediate subsurface restricted to the
294 centimetre to metre scale below the surface (A'Hearn et al., 2005; Thomas et al., 2008). This further
295 supports the notion that solar radiative heating penetrates to limited depths. Thus, the formation of
296 liquid water, if possible, will also be limited to depths of ~5cm<D<<1m.

297 **Non-conductive heating:** It is also worthwhile considering the role of non-conductive heat transfer
298 within the comet's subsurface as these processes may provide additional non-negligible heating
299 effects. Hu et al., (2019) explored the effects of radiative transfer and concluded that this is most
300 efficient in the shallow subsurface (~5cm), during daytime, at small heliocentric distances and in
301 materials with large pores. When compared against a purely conductive model radiative effects can
302 increase temperatures by at least +20°C (at a distance of 2 A.U. as modelled for 67P).

303 Other mechanisms are also possible. The sublimation of near-surface ice, for example, will generate
304 water vapour under an elevated pressure. Porous media-flow of water vapour inwards through the
305 pore network will also transfer heat inwards from the outer-layers, although this is generally
306 considered inefficient (Kömle and Steiner, 1992). Alternatively, freeze-thaw behaviour during diurnal
307 heating cycles may also enhance internal fracturing, allowing water vapour (or liquid water) to
308 penetrate deeper along open conduits. Attree et al., (2018) modelled the fracture behaviour of 67P
309 and suggested that cracks penetrating to depths of 0.25m into the surface are possible, consistent
310 with the observations of polygonal-shaped crack networks exposed on the comet's surface. Crack
311 networks in bodies which pass closer to the Sun than 67P are likely to penetrate deep and form more
312 extensive networks. Temperatures may, therefore, be somewhat higher than those suggested by
313 equation (eq.1).

314 **Rotational period and spin axis orientation:** Another major factor controlling the subsurface heating
315 is the rotational period of comets. Temperatures fluctuate rhythmically on a diurnal cycle – the
316 magnitude of which is greatest at the surface and decreases inwards. This temperature gradient is also
317 affected by a thermal time-lag due to the low thermal inertia of cometary materials (Wickramasinghe
318 et al., 2009; Farnham et al., 2013; Shi et al., 2016). For example, Farnham et al., (2013) observed that
319 jetting activity on 81P/Wild 2 continued for up to 4 hours after rotation of the jets into darkness. A

320 comet's rotational period therefore has significant control on the duration of subsurface heating and
321 the length of time liquid water can survive. Shorter rotational periods will necessarily result in shorter
322 episodes at peak temperatures (Wickramasinghe et al., 2009; Farnham et al., 2013; Shi et al., 2016).

323 Wickramasinghe et al., (2009) modelled a 40-hour rotation period (equivalent to that of 9P/Tempel
324 [Groussin et al., 2007]) and concluded that peak temperatures will be maintained for approximately
325 10 hours (one quarter day-length, Wickramasinghe et al., 2009). This timeframe is close to the
326 maximum rotational period measured for JFCs, which typically range between 8.1 hours and 17.2
327 hours (the interquartile range of rotational periods of 37 comets, calculated from the data given in
328 Kokotanekova et al., [2017], here displayed in Fig.5). Thus, for most comets which rotate faster, the
329 depth of heat penetration will also be shallower and the duration of heating shorter. Average
330 timescales for subsurface heating in periodic comets may therefore last just 2-5 hours per diurnal
331 cycle. However, the total duration over which liquid water could form (across repeated melting/re-
332 freezing events) will be a product of multiple daily cycles as the comet passes through perihelion.

333 Comets typically display significant activity for 1 month prior and 1-2 months after perihelion passage,
334 attesting to appreciable subsurface heating during this time (Lara et al., 2015; Snodgrass et al., 2016;
335 Pätzold et al., 2019). For example, 67P passed within 1.24 A.U. of the Sun on 13/08/2015 but displayed
336 enhanced coma activity for ~2 months with peak activity 2 weeks after perihelion (Snodgrass et al.,
337 2016). This indicates that the subsurface has a strong thermal lag and that average temperatures
338 increased slowly on week-long timescales creating a seasonal heating effect, even where diurnal
339 temperatures fluctuated over much shorter timescales (the rotational period of 67P is just 12.76
340 hours). Thus, it seems unavoidable that sustained subsurface heating occurs through the retention of
341 heat throughout the (short) night-time cooling phase in comets with stable rotating states and average
342 rotational periods. Peak temperatures could therefore be achieved either through combined
343 melting/re-freezing cycles or by a slow increase in subsurface temperature over seasonal timescales.
344 In both scenarios these conditions could exceed the 24-48 hours required for the aqueous alteration
345 of highly susceptible GEMS.

346 Comets can also have "tumbling" rotational states in which the orientation of the rotational axis varies
347 chaotically over time. In addition, a significant proportion of comets have stable rotational states but
348 high obliquity (axial tilt) resulting in strong seasonal contrasts and perihelion periods in which one
349 hemisphere experiences an enhanced heating effect due to longer exposure to solar heating. Among
350 the asteroid population most slow rotators (with periods in the 10's to 100's of hours) commonly have
351 tumbling rotational states (Harris and Pravec, 2005). Although the prevalence of chaotic rotational
352 states among periodic comets is poorly constrained, both stable and chaotic states have been
353 observed for several bodies. Notably, 1P and 67P have stable rotational axes, while both 17P and 46P
354 have chaotic states in which the axis of rotation changes even over the course of a single orbital period
355 (Mysen, 2004). Likewise, the rotational axis of 2P/Encke appears to have changed significantly over
356 the last 300 years (~100 orbits) with obliquity reaching an extreme value of 103° in ~1850 and later
357 remaining stable at ~70° between 1924-1984. During this time the spin axis was directed towards the
358 Sun, leaving a polar hemisphere continuously exposed during perihelion passes (Whipple and
359 Sekanina, 1979; Sekanina, 1988; Sanzovo et al., 2001). Similarly, the long-period comet C/1995 O1
360 (Hale-Bopp) also had an extreme axial tilt of 83° during its perihelion pass in 1996-97 (Licandro et al.,
361 1997). The effects of rotational period creating diurnal heating cycles may become irrelevant in bodies
362 with Sun-directed rotational axes, either due to tumbling rotation or high obliquity. In such situations
363 subsurface heat transfer is maximized generating more than sufficient time for alteration reactions to
364 proceed.

365 **(2) Pressure:** Internal gas pressures are generated by the sublimation of volatiles and super-volatiles.
366 The release of these gases raise local pore pressure as the gas release rate from mineral phases
367 exceeds the gas escape rate from the comet's subsurface (Prilank and Bar-Nun, 1990; Kömle et al.,
368 1992; Almedia et al., 2016). For liquid water to form, pressures must exceed the water triple point
369 (Fig.2), which requires pressures above 611Pa (at temperatures of 0°C) for pure water, and lower
370 pressures for impure/saline water (e.g. ~300 Pa at 2 mol% NaCl solution, Fig.2 and Feistel et al., 2008).

371 The existence of dusty ice-depleted crusts on comets which have been subject to multiple previous
372 perihelion degassing passages (Kömle et al., 1992; Wickramasinghe et al., 2009; Quirico et al., 2015)
373 and the presence of "dirty" ice, intermixed with other components appear to play a crucial role in the
374 formation of internal gas pressures.

375 Early estimates of cometary internal pressures were made by Prialnik and Bar-Nun (1990) using
376 numerical modelling to study the evolution of a comet's interior with a 1P/Halley-like orbit over
377 multiple perihelion passes. They assumed as a starting point a nucleus composed of cold porous
378 amorphous ice containing 10% trapped carbon monoxide and concluded that internal gas pressures
379 could potentially reach values as high as 2MPa when sublimating gases (released upon crystallization
380 of amorphous ice) become trapped. In their model peak pressures occur within 20m of the cometary
381 surface. However, Prialnik and Sierks (2017) produced a significantly revised model of internal gas
382 pressures and concluded that cometary peak pressures may be as low as 2Pa. This revised estimate is
383 constrained by the low material strength (especially under tensional stress) of cometary dust
384 aggregates, whose connections between clusters are exceptionally weak (Asphaug and Benz, 1996;
385 Blum et al., 2014).

386 Independently, Kömle et al., (1992) performed experimental studies heating cometary analogues
387 composed of porous fine-grained ice covered by a dark dust mantle composed of graphite and/or SiC
388 – representing a non-volatile crust covering an unheated pristine interior. They noted that the addition
389 of even small quantities of impurities radically changed the behaviour of the pore pressure within ice
390 structures. During sublimation the subsurface evolves significantly because small light-weight particles
391 are easily redistributed to block pore interconnections, allowing pressure build-up and creating larger
392 pores with fewer interconnections. However, these higher pressures were estimated to reach just
393 50Pa while also being restricted to a very thin boundary layer within the ice, most likely on the order
394 of millimetres to centimetres (Kömle et al., 1992). In contrast, deeper in the structure pore pressures
395 were consistent with the equilibrium vapour pressures.

396 A similar mechanism of raised internal gas pressure was also proposed by De Almedia et al., (2016) –
397 termed the pressurized obstructed pore model and based on outburst activity observed for
398 17P/Holmes. They suggested that after an initial heating phase and the sublimation of water-ice to
399 form water vapour, some of this vapour could refreeze before it escapes, thereby blocking pore space
400 and increasing the comet's tensile strength in or near the outer crust region. This would have the
401 effect of preventing the escape of newly released subsurface volatile gases. These trapped gases
402 would then ultimately be released in explosive episodes. Such a model could explain the observed
403 pre- and post-perihelion sudden explosive outburst activity. They estimate that internal gas pressures
404 on the order of 1kPa are required to facilitate rupture of the icy crust (De Almedia et al., 2016), while
405 Reach et a., (2010) estimated that the same explosion requires tensile strengths on length scales >10m
406 to be 10kPa<t<200kPa.

407 An alternative model for the evolution of cometary interiors was proposed by Miles (2016) and
408 explored how sublimating volatile species interact and could potentially work synergistically to
409 produce runaway heating and pressure increases. Miles (2016) suggests that an initial heating episode
410 results in the release of super-volatiles which raise the local pore pressures sufficiently to stabilise

411 simple hydrocarbon liquid phases, primarily liquid methane. Subsequent volatile gases which are
412 released then dissolve in this liquid methane forming a complex organic solution. Since these reactions
413 are exothermic this process acts as an internal heat “engine” and causes a progressive rise in internal
414 gas pressures and temperatures. Under this scenario it may therefore be possible to reach pressure-
415 temperature conditions far in excess of that required for liquid water stabilisation. Miles (2016)
416 estimates maximum pressures as high as 200kPa.

417
418 Although, the internal gas pressure estimates for cometary interiors vary widely, most studies
419 conclude that gas release from volatiles (when the comet approaches perihelion) occurs at rates
420 higher than the gas escape rate, primarily due to pore blocking below their non-volatile crusts. Thus,
421 the maximum internal pressures of comets are instead directly dependent on their tensile strength –
422 equivalent to their ability to withstand pressure before rupturing explosively. Estimates for cometary
423 tensile strength are more easily determined.

424
425 A rotating object is held together by material strength and gravitational forces. These resist the action
426 of centrifugal force that would otherwise catastrophically disrupt the object. Since centrifugal forces
427 are dependent on the rotation rate, fast spinning bodies and rotational breakup events provide unique
428 opportunities to investigate the tensile strength of comets. Such studies require accurate
429 measurement of a body’s size, shape and rotational period prior to breakup as well as estimates of
430 the object’s density and structure. They typically conclude that comets have low tensile strengths (20-
431 400Pa, Lisse et al. 1999; <100Pa Davidsson, 2001). Likewise, the fragmentation of D/1993 F2
432 (Shoemaker–Levy 9) by tidal forces as the comet passed within Jupiter’s Roche limit acted as a natural
433 experiment testing the tensile strength of a comet. The early breakup of Shoemaker–Levy 9 suggested
434 the comet had a loose aggregate structure and a low tensile strength (>270Pa, Greenberg et al., 1995).
435 By contrast, new observations from the Rosetta mission provide empirical evidence from an “*in-situ*”
436 comet. The presence of landslides and exposed steep cliffs formed under micro-gravity conditions also
437 suggest that 67P has very low tensile strength, potentially in the region of 3-15Pa, although upper
438 maximum values of 150Pa over 30m length scales and 1150Pa over 1m scales are quoted in Groussin
439 et al. (2015). Conversely, some of these slope features preserve evidence of fracturing (Sierks et al.,
440 2015), which necessarily requires non-zero tensile strengths. Alternatively, more direct estimates can
441 be made from the behaviour of the Philae lander, which hit the comet’s surface and encountered a
442 higher-than-expected compressive strength, estimated to be in the range 4-7MPa by Spohn et al.,
443 (2015) based on the incomplete penetration of the MUPUS (Multipurpose Sensors for Surface and
444 Sub-Surface Science) hammer. Since compressive strengths are typically an order of magnitude higher
445 than tensile strengths this suggests that the 67P parent body may support tensile strengths as high as
446 400-700kPa.

447
448 Data from 67P/Churyumov–Gerasimenko measures a “fresh” and dynamically young comet (Maquet,
449 2015). In contrast, the tensile strength of cometary materials may also evolve with heating, for
450 example due to the formation of re-frozen ice in the comet’s upper layers (Feaga et al., 2007; De
451 Almedia et al., 2016). Alternatively, if water vapour can lead to the hydration of silicates (Takigawa et
452 al., 2019) then the formation of interlocking clay minerals could also increase cometary tensile
453 strength by binding grains together. Initial formation of hydrous products from water vapour
454 alteration, even though incipient, is likely to lead to increases in strength owing to the formation of
455 hydrated minerals as a cement between touching mineral grains (Rhim, 2011). Similar behaviour is
456 observed in terrestrial sediments during early diagenesis where partial cements form on menisci
457 between mineral grains – this is particularly the case in beach sands where small amounts of cement
458 growth rapidly indurate unconsolidated sediment (Garrison, 1969). Observations of 67P/Churyumov–
459 Gerasimenko may not, therefore, provide the most appropriate values of tensile strength in relation
460 to liquid water generation since phyllosilicates were not detected on this comet. Alternative estimates
461 for tensile strength have been derived from cometary meteoroids, they have values between 10kPa
462 from pristine comets and significantly higher values of 80kPa for evolved comets (such as the taurids

463 from 2P/Encke) (Trigo-Rodriguez and Blum, 2009). These values support the notion that tensile
464 strength increases with the time spent in the inner solar system. The tensile strength of cometary
465 materials, therefore, may exceed the ~300-600Pa required for liquid water stabilisation and
466 demonstrate that conditions suitable to liquid water could be supported in the cometary interior
467 without disruption (Fig.6 summarizes temperature and pressure estimates for periodic comets
468 discussed in section 5).

469

470 **6. Alternative mechanisms for the existence of liquid water**

471

472 In section 5 we considered the viability of pure liquid water within a cometary subsurface forming
473 under equilibrium conditions. However, there are additional factors that could facilitate the
474 generation and survival of liquid water at lower temperatures and lower pressures under dynamic
475 conditions. These include (1) the addition of salts to form cryobrines (2) the existence of nano-scale
476 liquid water films and (3) the formation of liquid water under non-equilibrium conditions.

477

478 (1) Although pure water requires conditions to exceed $T=0.01^{\circ}\text{C}$ and $P=611.2\text{Pa}$, impure water can
479 exist at lower temperatures and pressures owing to the effects of freezing point depression (Fig.2).
480 For simple $\text{H}_2\text{O}-\text{NaCl}$ systems, moderate quantities of salt can lower the eutectic (-8°C) and half the
481 required vapour pressure ($\sim 300\text{Pa}$) (Feistel et al., 2008). In the extreme case concentrated cryo-brines
482 containing both Cl-bearing and S-bearing salts can support remarkably low eutectic points, stable
483 down to temperatures as low as -63°C and pressures as low as 100 Pa (Brass, 1980; Chevrier and
484 Altheide, 2008; Möhlmann, 2011). The relevance of such highly concentrated solutions for cometary
485 systems remains unknown but seem likely, given that both sulphur and chlorine are liberated early in
486 the aqueous alteration of chondritic materials; sulphur is released from GEMS and GEMS-like phases,
487 while chlorine is leached from chondrule glass (Brearley and Jones, 2018). These highly saline
488 conditions may therefore be present after an initial period of liquid water formation, where an actively
489 evaporating solution leaves behind an increasingly concentrated brine. In such cases, salt
490 concentration by evaporation would act to increase the length of time at which liquid water remains
491 through freezing point depression.

492

493 (2) At the micron to nano-scale, small quantities of undercooled interfacial water can form and survive
494 where the attractive pressure of van der Waals forces between mineral grain surfaces acts to stabilize
495 water films (Rietmeijer, 1985; Möhlmann, 2011). This occurs because intermolecular forces between
496 grains generate sufficient pressure to cause freezing point depression. Thus, liquid water will be
497 generated (and maintained permanently) where silicate and ice grains are in contact. Experimental
498 studies demonstrate that a thin layer ($>6\text{\AA}$) of this surface water can never be frozen even as
499 temperatures approach absolute zero (Anderson, 1968; Rietmeijer, 1985). Furthermore, the thickness
500 of the adsorbed water varies dependent on temperature and mineral species, with higher
501 temperatures (close to the system's melting point) and hydrophilic minerals capable of maintaining
502 thicker films. In fine-grained mixed mineral-ice assemblages liquid water content, generated by
503 interfacial forces, can reach up to 10% of the total water present (Möhlmann, 2011).

504

505 Cometary micrometeorites are composed of submicron mineral assemblages with high porosities.
506 Some of this porosity would have been filled by water-ice, creating situations in which interfacial liquid
507 water would form and could theoretically perform aqueous alteration reactions (Rietmeijer, 1985).
508 However, these conditions will necessarily occur at low temperatures, below the freezing point of the
509 water-ice system (for the ambient pressure conditions) and thus reaction rates will be exceptionally
510 slow (perhaps on the order of 10^4 - 10^6 years, Rietmeijer, 1985). These long timescales are not relevant
511 for perihelion-induced alteration mechanisms but potentially important processes in long-period
512 comets. Furthermore, even where reactions are viable their extent is also limited. In the case of silicate
513 alteration reaction rates slow significantly once the exposed mineral face has been altered. This is
514 because the reaction products create a barrier to diffusion, limiting further alteration below the

515 exposed surface (Rietmeijer et al., 2002; Le Guillou et al., 2015). Thus, Interfacial liquid water may
516 produce localized alteration, along grain surfaces in direct contact with water-ice. However, such
517 conditions could not generate extensive aqueous alteration nor are they likely responsible for the
518 moderately altered chondritic porous micrometeorites which do not appear to show correlation
519 between pore space proximity and alteration extent. (Fig.4, [Noguchi et al., 2017](#)). Instead interfacial
520 water may be capable of generating subtle nanophase alteration products like the ~300nm amphibole
521 grains suspended within a GEMS host that were described by Busemann et al., ([2009 \[Fig.8\]](#)) within a
522 cometary micrometeorite.

523

524 (3) For time-variable conditions the temporary existence of liquid water is also possible at
525 temperatures and pressures well beyond the triple point. This was demonstrated experimentally by
526 Kömle et al., ([2018](#)) where a melting probe slowly penetrated into a water-ice layer under ambient
527 pressures of just 20Pa and temperatures between -10°C to -30°C. Such situations might be relevant
528 to scenarios where a cometary parent body is impacted, either on the micron-scale by high-speed
529 cosmic dust or on larger scales by centimetre to metre sized objects. Temperature and pressures
530 generated would then easily exceed triple point requirements. However, the lifetimes of liquid water
531 under such conditions are unlikely to survive longer than a few minutes. Non-equilibrium liquid water
532 is therefore not expected to be a significant mechanism for aqueous alteration reactions.

533

534 **7. Is alteration possible before dust shedding?**

535

536 Previously we explored how heating over multiple diurnal cycles could produce repeated melting and
537 re-freezing events as well as a slow increase in the average subsurface temperature. However,
538 cumulative heating will only be possible if the erosion rate at the comet's surface near perihelion is
539 sufficiently slow for alteration to occur before the shallow subsurface is ejected into the coma. It is
540 therefore critical to consider how much material may be lost from the comet's surface during a single
541 perihelion pass.

542

543 Estimates of the mass loss rate for comets over a single perihelion pass are variable, reflecting our
544 limited knowledge of the process as well as the complex set of parameters which combine to control
545 the mass loss rate. Based on the Deep Impact observations of 9P/Tempel Thomas et al., ([2008](#)) argued
546 that the peak erosion rate for periodic comets can reach rates as high as one thermal skin depth per
547 cometary day. This translates to a loss of around 3m per orbit (for 9P) equivalent to approximately
548 100 thermal skin depths (assuming a skin depth of just 2-3cm). However, a comet's surface erosion
549 rate is strongly dependent on several factors, not just the thermal skin depth but also the depth from
550 which volatile gas emissions occur as well as the thickness of the non-volatile cover. As these factors
551 increase the rate of erosion may be slowed by a factor of ten. Alternative estimates generally suggest
552 lower erosion rates. Bertaux ([2015](#)) estimated a loss rate of 1.0 ± 0.5 m per orbit for 67P using space
553 telescope data collected over its three previous orbits (1996, 2002, and 2009) prior to arrival of the
554 Rosetta spacecraft. In contrast, during the 2015 perihelion Rosetta data suggest that 67P lost just 0.1%
555 of its nucleus mass ([Pätzold et al., 2019](#)) translating to an erosion rate of 0.44-0.55m averaged across
556 the surface ([Keller et al., 2017](#)). Meanwhile Sanzovo et al., ([2001](#)) estimated relatively modest erosion
557 rates for two comets: 6P/d'Arrest (~0.5m per orbit) and 2P/Encke (~0.3m per orbit). In Fig.7 we
558 compare how differences in the erosion rate (100cm, 50cm, 30cm and 10cm per orbit) and the
559 duration over which the total surface loss occurs (x-axis titled as "perihelion duration" [and given in
560 weeks]) affect the averaged surface erosion rate. This demonstrates that even at moderate-to-high
561 erosion rates of 100cm/perihelion and a short duration over which this loss occurs (1 week), the
562 outermost 10cm of a comet can survive for ~16.8 hours (Fig.7). Furthermore, as the duration over
563 which surface loss occurs is increased or the erosion rate decreases, this outermost layer survives for
564 much longer. These calculations suggest that in some periodic comets the conditions of liquid water
565 could be maintained long enough to result in the aqueous alteration of GEMS to primitive
566 phyllosilicates.

567

568 **8. Spectroscopic observations of phyllosilicate-bearing comets**

569 Ground-based and space-based remote sensing observations of aqueous alteration products in
570 comets are somewhat controversial. Hayward et al., (2000) and Kelley and Wooden (2009) failed to
571 detect hydrated spectral signatures associated with phyllosilicates in two comets, suggesting these
572 are not major components on cometary surfaces. If aqueous alteration minerals are present, they are
573 therefore highly limited in extent. This is consistent with the conclusions from microanalysis studies
574 of cometary micrometeorites. When phyllosilicates are present, they occur at low concentrations and
575 have poorly crystalline structures (Noguchi et al., 2017). However, two other comets (9P/Tempel and
576 Hale-Bopp [C/1995 O1]) have reported detections of both carbonate and (probable) phyllosilicate
577 (Lisse et al., 2006; 2007) and notably both comets passed close to the Sun (1.542 and 0.914 AU
578 respectively). The carbonate emission especially occurs in a "clean" part of the mid-infrared spectrum
579 unconfused by other possible sources of emission. Additionally, outburst jets from 1P/Halley showed
580 evidence of carbonate spectral signatures (Bregman et al., 1987). Since outbursts are characterized by
581 sudden enhanced dust release without concurrent increases in gas production, they may be
582 associated with landslide activity (Pajola et al., 2017) releasing materials from the immediate
583 subsurface. Bussemann et al. (2009) added support to the presence of carbonate in comets through
584 the discovery of carbonate grains in IDPs collected during the Pi Puppids meteor shower and
585 associated with comet 26P/Grigg-Skjellerup – this makes the current evidence for cometary
586 carbonates relatively strong.

587 **Phyllosilicates on 9P/Tempel:** NASA's *Deep Impact* mission collided with the nucleus of comet
588 9P/Tempel and generated a large plume of material excavated from the comet's subsurface
589 (generating a crater ~200m in diameter and removing material potentially to a depth of 5m [Schultz
590 et al., 2013]). Spectral observations by the Spitzer Space Telescope interpreted by Lisse et al., (2006;
591 2007) suggested the presence of both carbonates (occurring at ~5% of the ejecta by surface area) and
592 phyllosilicates (composing ~8% of the ejecta by surface area). Since both these minerals are strongly
593 associated with aqueous alteration, this provides a compelling case that liquid water existed within
594 the subsurface of 9P at some point, either during the early solar system, or recently due to perihelion
595 heating. Although the detection of a phyllosilicate spectral signature among the impact debris of 9P
596 remains controversial (e.g. Harker et al., 2005) its presence would be consistent with a subsurface
597 liquid water generation model.

598 Dynamical modelling suggests that 9P/Tempel's orbit evolved during the 1600's after a close-approach
599 with Jupiter, resulting in a significant decrease in the body's perihelion distance from ~3.5 A.U. to 1.5
600 A.U. (Yeomans et al., 2004). This would significantly increase the comet's subsurface heating and
601 resulting activity, ultimately leading to its discovery in 1867.

602 **Phyllosilicates on Halle-Bopp:** Hale-Bopp is another comet in which a probable phyllosilicate spectral
603 signature has been identified. Lisse et al., (2007) argue for abundances around 18%. In contrast,
604 Wooden et al., (1999) could not rule out the possibility of phyllosilicates in the spectra of Hale-Bopp
605 but limited their abundance to <1%. Similarly, Hale-Bopp's orbital history is more uncertain. It is
606 dynamically young but with an exceedingly long orbital period, approximately 2500 years. Hale-Bopp
607 may have been perturbed by close-approach with Jupiter approximately 4200 years ago (2215 BCE),
608 which led to a significant reduction in its perihelion down to ~0.9A.U. (Mardsen, 1997). Hale-Bopp has
609 likely experienced far fewer close perihelia than 9P/Tempel although its single known pass generated
610 significant cometary activity resulting in sufficient brightness for unaided naked eye observations over
611 18 months (1996-1997, de Almeida et al., 2009).

612 To date, 9P/Tempel and Hale-Bopp remain the only comets with potential phyllosilicate spectral
613 signatures and thus evidence of pronounced aqueous alteration. Tempel 1 has resided within 225
614 million km of the Sun (~1.5 A.U.) and remained in this close-approach orbit for over 400 years
615 (equivalent to more than 70 perihelion passes) – providing a long duration over which repeated
616 surface heating of the comet’s outer layers could trigger aqueous alteration. For comparison, the
617 anhydrous comet WILD 2 (81P/Wild) was only brought into the inner solar system recently, after a
618 close-approach with Jupiter in September 1974 (Królikowska and Szutowicz, 2006). Thus, when this
619 body was sampled by the STARDUST mission in 2006, relatively few perihelia had passed (~5 orbits),
620 limiting the potential for radiative heating. Similarly, 67P/Churyumov–Gerasimenko’s orbit evolved
621 following a close-approach with Jupiter in 1959, leading to a significant reduction in its perihelion
622 distance from 2.7A.U. to 1.3A.U. (Maquet, 2015). Thus, the lack of hydrated phyllosilicates on 67P is
623 expected given its (solar-facing) daytime temperatures do not appear to exceed -45°C (Tosi et al.,
624 2019) and it has experienced relatively few (<10) perihelion passes at this closer distance. This
625 suggests that perihelion-induced alteration can only be effective for comets which are thrown into the
626 inner solar system and spend several perihelia close (<1.5A.U.) to the Sun.

627 **9. Implications – How many comets are affected by perihelion-induced liquid water** 628 **formation?**

629 Most known periodic comets have perihelion distances <4A.U. (Fig.8, 348 bodies or >95%, [Minor](#)
630 [Planet Center, 2019](#)). If alteration by liquid water is facilitated by an initial phase of vapour-driven
631 alteration in order to increase a comet’s tensile strength and lower surface permeability thereby
632 allowing the comet to sustain higher internal gas pressures sufficient for the stabilization of liquid
633 water, then the initial stages of alteration are likely to begin at temperatures of ~0°C. The data in Fig.6
634 suggest that this threshold is met between 1.0-1.5 A.U. Using a threshold of 1.5. A.U. suggests
635 alteration might occur on approximately 91 known periodic comets (24.8% of the known population).
636 Alternatively, if a threshold of <1 A.U. is required then approximately 35 known periodic comets (9.5%
637 of the population) may be affected by this mechanism. However, because rotational properties also
638 appear to exert a strong control, these two factors act together to prevent perihelion-induced
639 alteration being a widespread phenomenon among the periodic comet population. Today the
640 rotational properties of most periodic comets are unstudied. This makes estimating the number of
641 bodies affected by this alteration mechanism difficult. Assuming one third of periodic comets have
642 either a high obliquity (creating a sun-directed hemisphere) or slow rotational period, and that
643 distances <1.5 or <1.0 A.U. are required, this suggests that 3-9% of periodic comets may be able to
644 generate subsurface liquid water during perihelion and perform aqueous alteration reactions.

645 Considering the extremes, eight known periodic comets pass within 0.5A.U. of the Sun. They include
646 249P/LINEAR, 23P/Brorsen-Metcalf, 2P/Encke and 96P/Machholz as well as four SOHO (Solar and
647 Heliospheric Observatory) comets (321P/SOHO, 322P/SOHO, 323P/SOHO and 342P/SOHO). Comets
648 which pass exceptionally close to the Sun are termed sungrazers although the strict definition requires
649 perihelia of $\lesssim 0.014$ A.U., while a looser definition of “sunskirters” is used to describe comets identified
650 by the SOHO spacecraft, which by necessity of their discovery method must pass close to the Sun
651 ($\ll 0.5$ A.U., [Battams and Knight, 2017](#)). By May 2016, there were 3138 sunskirters, recently
652 discovered, with poorly-constrained orbits and not currently assigned as “periodic” comets due to the
653 lack of a second observed perihelion pass (or second apparition) ([Battams and Knight, 2017](#)). The
654 sunskirters are primarily members of the Kreutz comet family, characterised by perihelia <2 solar radii,
655 high orbital inclinations ($i \sim 140^\circ$) and long orbital periods. They may represent a single large parent
656 body which broke up during a close-approach due to extreme tidal forces ([Davidsson, 2001](#); [Sekanina,](#)
657 [2002](#)). Comet 2P/Encke as well as the sunskirting comets are ideal candidates for perihelion-induced

658 aqueous alteration, representing the most likely candidates in which to detect advanced alteration on
659 a cometary petrology.

660 **Sourcing micrometeorites to Earth:** Finally, we note that numerous periodic comets with small
661 perihelia (<1.4A.U.) are major dust-producing bodies associated with active meteor showers (perhaps
662 as many as 42 candidate comets, [Jenniskens, 2008](#)). Notably this population includes the Pi Puppids
663 linked to 26P/Grigg-Skjellerup whose perihelion is 1.1 A.U., the Draconids linked to 21P/Giacobini-
664 Zinner whose perihelion is 1.038 A.U., the Perseids linked to 109P/Swift-Tuttle whose perihelion is
665 0.96 A.U and the Orionids and Eta Aquariids linked to 1P/Halley whose perihelion is 0.586A.U.
666 ([Jenniskens and Jenniskens, 2006](#); [Jenniskens, 2008](#)). In addition, the active asteroid 3200 Phaethon –
667 the target of JAXA’s planned DESTINY+ mission – also has an exceptionally small perihelion distance
668 (just 0.14A.U) and is likewise associated with the Geminids meteor stream ([Jewit and Li 2010](#)).
669 Estimated surface temperatures near perihelion may reach >900°C based on numerical modelling
670 ([Chaumard et al., 2012](#)). This large group of comets are predominantly dormant bodies, which no
671 longer experience major cometary activity but remain associated with their daughter meteoroid
672 streams ([Jenniskens, 2008](#)). By virtue of this association between meteor showers and dormant near-
673 Earth comets, they will clearly contribute significantly to the sources of micrometeoroids reaching
674 Earth ([Jenniskens 2008](#)). However, much of this dust will have high entry velocities owing to their
675 eccentric orbits (generally between 25-70kms⁻¹, [Younger et al., 2012](#)) and thus only a small fraction of
676 grains from this population – those with the most favourable entry conditions (small sizes and low
677 entry angles) – will survive atmospheric entry ([Flynn, 1990](#); [Love and Brownlee, 1991](#)) to be recovered
678 either in the stratosphere by high-altitude collection missions ([Flynn, 1994](#)) or from the Earth’s surface
679 (e.g. in Antarctic snow) and subsequently analysed. However, a micrometeorite suspected to belong
680 to the Pi-Puppids meteor shower (~19kms⁻¹, [Vaubaillon and Colas, 2005](#)), associated with 26P/Grigg-
681 Skjellerup was recovered and studied by Busemann et al., ([2009](#)) – this particle contained both
682 carbonates and amphibole (commonly considered secondary alteration minerals). Thus, the relatively
683 rare mildly altered chondritic porous micrometeorites described by Noguchi et al., ([2015](#); [2017](#)) and
684 ultracarbonaceous micrometeorites ([Yabuta et al., 2017](#)) could be direct samples of these near-Earth
685 heated comets.

686 In contrast, cometary dust originating from more distant comets, those with larger perihelion
687 distances and which have not experienced perihelion-induced aqueous alteration are likely to supply
688 significantly more dust to Earth’s surface due to a strong survivorship bias. This low eccentricity long-
689 period population produce cosmic dust whose orbits are progressively circularized, evolving to low
690 eccentricities and lower speeds (relative to Earth’s orbit) meaning that they are more likely to survive
691 atmospheric entry and are thus expected to appear more abundant in micrometeorite collections
692 ([Nesvorný et al., 2010](#); [Carrillo-Sánchez et al., 2015](#); [2016](#)). This effect could generate an
693 overabundance of cosmic dust from unaltered comets among our micrometeorite collections.

694 **10. Conclusions**

695 Nominally anhydrous chondritic porous micrometeorites and ultracarbonaceous Antarctic
696 micrometeorites are widely considered to be samples of comets. Some of these particles show
697 evidence of mild parent body aqueous alteration ([Nouguchi et al., 2015](#); [2017](#); [Yabuta et al., 2017](#)),
698 characterised by variable degrees of hydration resulting in the conversion of amorphous GEMS
699 (primitive solar system condensates) to low crystallinity Fe-rich phyllosilicates. This incipient
700 alteration, without further processing requires extremely short exposure to liquid water, most likely
701 on timescales <24hrs, under mildly alkaline conditions (>pH8) and at low temperatures (≈0°C), as
702 demonstrated by experimental studies ([Rietmeijer et al., 2004](#); [Nakamura-Messenger et al., 2011](#)). In

703 contrast, in-situ observations of comets from spectroscopic telescopes (Kelley and Wooden, 2009) and
704 space missions (Zolensky et al., 2006; 2008) conclude that cometary mineralogies lack evidence of
705 phyllosilicates and are anhydrous – with the possible exception of 9P/Tempel and Hale-Bopp (Lisse et
706 al., 2006). Heat sources conventionally considered responsible for aqueous alteration in asteroidal
707 settings – namely radiogenic heating (Keil, 2000; McSween et al., 2002) and impact heating (Rubin,
708 2012; Hanna et al., 2015; Lindgren et al., 2015; Vacher et al., 2018) – are expected to be unsuitable
709 mechanisms for alteration on late-formed outer solar system cometary parent bodies (Davidsson et
710 al., 2016; Mousis et al., 2017). Thus, a different energy source is required to explain the observed
711 alteration of cosmic dust.

712 We explored the viability of perihelion solar radiative heating as the energy source for aqueous
713 alteration. This was previously suggested by Rietmeijer et al., (2004); Wickramasinghe et al., (2009),
714 Ohtsuka et al., (2009) and Nakamura-messenger et al., (2011). Using recent experimental work,
715 numerical modelling, space mission data and microanalysis studies, we explored whether the short-
716 term generation of liquid water within the cometary subsurface during close-approaches to the Sun
717 was possible. We conclude that solar radiative heating may be capable of generating liquid water in a
718 comet's immediate subsurface for selected bodies with favourable conditions.

719 Based on the spacecraft-measured surface temperatures of comets 1P, 9P, 19P, 67P and 103P and
720 their relationship with perihelion distance we demonstrated that bodies orbiting within <1.5 A.U. of
721 the Sun can generate sufficiently high temperatures for liquid water to form in their immediate
722 subsurface (at depths <40cm and likely <10cm). In contrast, whether sufficient pressure can be
723 generated to stabilize liquid water remains uncertain. Previous studies have suggested a wide range
724 of internal gas pressures, ranging over 5 orders of magnitude (1-700kPa). Alternatively, if we assume
725 that the presence of explosive eruptions, as observed for several comets (Priolnik and Bar-Nun, 1992;
726 de Almeida et al., 2016) is evidence that gas pressures can exceed the tensile strength of cometary
727 material, which are generally on the order of 1000's of Pascals (Trigo-Rodriguez and Blum, 2009;
728 Spohn et al., 2015), this suggests sufficient pressure could be generated.

729 Based on orbital data, approximately 9-24% of periodic comets pass within 1.0A.U. or 1.5 A.U. of the
730 Sun. This provides an upper limit to the total number of bodies that may be affected by perihelion-
731 induced heating. However, because many of these bodies are expected to have stable rotational axes
732 and short rotational periods (<20 hours), subsurface heating durations in most comets may be too
733 short to produce appreciable alteration. Instead, we predict that perihelion-induced aqueous
734 alteration is likely only effective in comets with small perihelia and favourable rotational states (slow
735 periods or Sun-directed axes). Given these limitations we predict that this mechanism should affect 3-
736 9% of the current periodic comet population.

737 However, the fate of all comets is either evaporation, collisional disruption or ejection from the solar
738 system. Many of the known periodic comets currently with distant perihelia are likely to be perturbed
739 inwards, entering the zone of viable perihelion-induced aqueous alteration. On longer timescales, the
740 inner solar system comet population is continually renewed by comets sent from the Kuiper belt and
741 Oort cloud, providing a steady stream of material to replace those evaporated by the Sun. Thus, many
742 more comets than those currently inside the potential zone of alteration will be affected, making this
743 mechanism an important process in the end-stages of comet lifetimes.

744 Today, comet 2P/Encke represents an ideal candidate for perihelion-induced aqueous alteration
745 reactions, having a small perihelion (~0.3 A.U.), a short orbital period (3.3 years) and a chaotic
746 rotational state in which the Northern hemisphere is known to have been exposed continuously to
747 solar heating for multiple orbital periods for over at least 100 years (Whipple and Sekanina, 1979).
748 Furthermore, 2P/Encke is the parent body of the Taurids meteor shower and therefore sources

749 abundant cometary dust to Earth, raising the probability that aqueously altered cometary
750 micrometeorites derived from a solar-heated body should be present among micrometeorite
751 collections.

752 **11. Acknowledgements**

753 This work was funded by both UK and Italian research grants: In the UK, by the Science and Technology Facilities
754 Council (STFC), through grant ST/R000727/1 (MDS and SSR) and grant ST/J001260/1 (MJG). In Italy, by grants
755 MIUR: PNRA16_00029 and PRIN2015_20158W4JZ7 (MDS and LF). We thanks Cecile Engrand for insightful
756 comments regarding the alteration of GEMS. We thank Norbert Kömle and an anonymous reviewer for their
757 helpful comments during the review stage and Associate Editor Michael Combi for handling of this manuscript.

758 **12. References**

- 759 1. A'Hearn, M.F., Belton, M.J.S., Delamere, W.A., Kissel, J., Klaasen, K., McFadden, L.A., Meech, K.J., Melosh,
760 H.J., Schultz, P.H., Sunshine, J.M. and Thomas, P.C., 2005. Deep impact: excavating comet Tempel 1. *Science*,
761 310:258-264, doi:10.1126/science.1118923.
- 762 2. Anderson, D.M., 1968. Undercooling, freezing point depression, and ice nucleation of soil water. *Israel*
763 *journal of Chemistry*, 6:349-355, doi:10.1002/ijch.196800044.
- 764 3. Asphaug, E. and Benz, W., 1996. Size, density, and structure of Comet Shoemaker–Levy 9 inferred from the
765 physics of tidal breakup. *Icarus*, 121:225-248, doi:10.1006/icar.1996.0083.
- 766 4. Attree, N., Groussin, O., Jorda, L., Rodionov, S., Auger, A.T., Thomas, N., Brouet, Y., Poch, O., Kührt, E.,
767 Knapmeyer, M. and Preusker, F., 2018. Thermal fracturing on comets-Applications to 67P/Churyumov-
768 Gerasimenko. *Astronomy & Astrophysics*, 610, doi:10.1051/0004-6361/201731937.
- 769 5. Battams, K. and Knight, M.M., 2017. SOHO comets: 20 years and 3000 objects later. *Philosophical*
770 *Transactions of the Royal Society A: Mathematical, Physical and Engineering Sciences*, 375:20160257,
771 doi:10.1098/rsta.2016.0257.
- 772 6. Berger, E.L., Zega, T.J., Keller, L.P. and Lauretta, D.S., 2011. Evidence for aqueous activity on comet 81P/Wild
773 2 from sulfide mineral assemblages in Stardust samples and CI chondrites. *Geochimica et Cosmochimica*
774 *Acta*, 75:3501-3513, doi:10.1016/j.gca.2011.03.026
- 775 7. Berger, E.L., Keller, L.P. and Lauretta, D.S., 2015. An experimental study of the formation of cubanite
776 (CuFe₂S₃) in primitive meteorites. *Meteoritics & Planetary Science*, 50:1-14, doi:10.1111/maps.12399.
- 777 8. Bertaux, J.L., 2015. Estimate of the erosion rate from H₂O mass-loss measurements from SWAN/SOHO in
778 previous perihelions of comet 67P/Churyumov-Gerasimenko and connection with observed rotation rate
779 variations. *Astronomy & Astrophysics*, 583, doi:10.1051/0004-6361/201525992.
- 780 9. Biver, N., Bockelee-Morvan, D., Colom, P., Crovisier, J., Davies, J.K., Dent, W.R., Despois, D., Gerard, E.,
781 Lellouch, E., Rauer, H. and Moreno, R., 1997. Evolution of the outgassing of Comet Hale-Bopp (C/1995 O1)
782 from radio observations. *Science*, 275:1915-1918, doi:10.1126/science.275.5308.1915.
- 783 10. Blum, J., Gundlach, B., Mühle, S. and Trigo-Rodriguez, J.M., 2014. Comets formed in solar-nebula
784 instabilities!—An experimental and modeling attempt to relate the activity of comets to their formation
785 process. *Icarus*, 235:156-169, doi:10.1016/j.icarus.2014.03.016.
- 786 11. Bradley, J.P., 1994. Chemically anomalous, preaccretionally irradiated grains in interplanetary dust from
787 comets. *Science*, 265:925-929, doi:10.1126/science.265.5174.925.
- 788 12. Bradley, J.P., 2019. GEMS and the devil in their details. *Nature Astronomy*, 3:603-605, doi:10.1038/s41550-
789 019-0833-9.
- 790 13. Brass, G.W., 1980. Stability of brines on Mars. *Icarus*, 42:20-28, doi:10.1016/0019-1035(80)90237-7.
- 791 14. Brearley, A.J. and Jones, R.H., 2018. Halogens in chondritic meteorites. In *The Role of Halogens in Terrestrial*
792 *and Extraterrestrial Geochemical Processes* (pp. 871-958). Springer, Cham.
- 793 15. Bregman, J.D., Campins, H., Witteborn, F.C., Wooden, D.H., Rank, D.M., Allamandola, L.J., Cohen, M. and
794 Tielens, A.G., 1988. Airborne and groundbased spectrophotometry of Comet P/Halley from 5–13
795 micrometers. In *Exploration of Halley's Comet* (pp. 616-620). Springer, Berlin, Heidelberg.

- 796 16. Bockelée-Morvan, D., Debout, V., Erard, S., Leyrat, C., Capaccioni, F.A.B.R.I.Z.I.O., Filacchione,
797 G.I.A.N.R.I.C.O., Fougere, N., Drossart, P., Arnold, G., Combi, M. and Schmitt, B., 2015. First observations of
798 H₂O and CO₂ vapour in comet 67P/Churyumov-Gerasimenko made by VIRTIS onboard Rosetta. *Astronomy*
799 *& Astrophysics*, 583, doi:10.1051/0004-6361/201526303.
- 800 17. Buchanan, J.Y., 1888. 2. On Ice and Brines. *Proceedings of the Royal Society of Edinburgh*, 14:129-147,
801 doi:10.1017/S0370164600003667.
- 802 18. Busemann, H., Nguyen, A.N., Cody, G.D., Hoppe, P., Kilcoyne, A.D., Stroud, R.M., Zega, T.J. and Nittler, L.R.,
803 2009. Ultra-primitive interplanetary dust particles from the comet 26P/Grigg–Skjellerup dust stream
804 collection. *Earth and Planetary Science Letters*, 288:44-57, doi:10.1016/j.epsl.2009.09.007.
- 805 19. Carrillo-Sánchez, J.D., Plane, J.M.C., Feng, W., Nesvorný, D. and Janches, D., 2015. On the size and velocity
806 distribution of cosmic dust particles entering the atmosphere. *Geophysical research letters*, 42:6518-6525,
807 doi:10.1002/2015GL065149.
- 808 20. Carrillo-Sánchez, J.D., Nesvorný, D., Pokorný, P., Janches, D. and Plane, J.M.C., 2016. Sources of cosmic dust
809 in the Earth's atmosphere. *Geophysical research letters*, 43:11-979, doi:10.1002/2016GL071697.
- 810 21. Chaumard, N., Devouard, B., Delbo, M., Provost, A. and Zanda, B., 2012. Radiative heating of carbonaceous
811 near-Earth objects as a cause of thermal metamorphism for CK chondrites. *Icarus*, 220:65-73,
812 doi:10.1016/j.icarus.2012.04.016.
- 813 22. Chevrier, V.F. and Altheide, T.S., 2008. Low temperature aqueous ferric sulfate solutions on the surface of
814 Mars. *Geophysical Research Letters*, 35, doi:10.1029/2008GL035489
- 815 23. Choi, Y.J., Cohen, M., Merk, R. and Prialnik, D., 2002. Long-term evolution of objects in the Kuiper Belt
816 zone—Effects of insolation and radiogenic heating. *Icarus*, 160:300-312.
- 817 24. Davidsson, B.J., 2001. Tidal splitting and rotational breakup of solid biaxial ellipsoids. *Icarus*, 149:375-383,
818 doi:10.1006/icar.2000.6540.
- 819 25. Davidsson, B.J., Gutiérrez, P.J., Groussin, O., A'Hearn, M.F., Farnham, T., Feaga, L.M., Kelley, M.S., Klaasen,
820 K.P., Merlin, F., Protopapa, S. and Rickman, H., 2013. Thermal inertia and surface roughness of Comet
821 9P/Tempel 1. *Icarus*, 224:154-171, doi:10.1016/j.icarus.2013.02.008.
- 822 26. Davidsson, B.J.R., Sierks, H., Güttler, C., Marzari, F., Pajola, M., Rickman, H., A'Hearn, M.F., Auger, A.T., El-
823 Maarry, M.R., Fornasier, S. and Gutiérrez, P.J., 2016. The primordial nucleus of comet 67P/Churyumov-
824 Gerasimenko. *Astronomy & Astrophysics*, 592:A63, doi:10.1051/0004-6361/201526968.
- 825 27. de Almeida, A.A., Boczeko, R., Sanzovo, G.C. and Sanzovo, D.T., 2009. Analysis of total visual and CCD V-
826 broadband observations of Comet C/1995 O1 (Hale-Bopp): 1995–2001. *Advances in Space Research*, 44:335-
827 339, doi:10.1016/j.asr.2009.03.028.
- 828 28. de Almeida, A.A., Boice, D.C., Picazzio, E. and Huebner, W.F., 2016. Water outburst activity in Comet
829 17P/Holmes. *Advances in Space Research*, 58:444-452, doi:10.1016/j.asr.2016.05.001.
- 830 29. de Leuw, S., Rubin, A.E., Schmitt, A.K. and Wasson, J.T., 2009. 53Mn–53Cr systematics of carbonates in CM
831 chondrites: Implications for the timing and duration of aqueous alteration. *Geochimica et Cosmochimica*
832 *Acta*, 73:7433-7442, doi:10.1016/j.gca.2009.09.011.
- 833 30. Dobrică, E. and Brearley, A.J., 2014. Widespread hydrothermal alteration minerals in the fine-grained
834 matrices of the Tieschitz unequilibrated ordinary chondrite. *Meteoritics & Planetary Science*, 49:1323-1349,
835 doi:10.1111/maps.12335.
- 836 31. Dobrică, E., Engrand, C., Duprat, J., Gounelle, M., Leroux, H., Quirico, E. and Rouzaud, J.N., 2009. Connection
837 between micrometeorites and Wild 2 particles: From Antarctic snow to cometary ices. *Meteoritics &*
838 *Planetary Science*, 44:1643-1661, doi:10.1111/j.1945-5100.2009.tb01196.x.
- 839 32. Duprat, J., Dobrică, E., Engrand, C., Aléon, J., Marrocchi, Y., Mostefaoui, S., Meibom, A., Leroux, H., Rouzaud,
840 J.N., Gounelle, M. and Robert, F., 2010. Extreme deuterium excesses in ultracarbonaceous micrometeorites
841 from central Antarctic snow. *Science*, 328:742-745, doi:10.1126/science.1184832.
- 842 33. Emerich, C., Lamarre, J.M., Moroz, V.I., Combes, M., Sanko, N.F., Nikolsky, Y.V., Rocard, F., Gispert, R., Coron,
843 N. and Bibring, J.P., 1986, December. Temperature and size of the nucleus of Halley's Comet deduced from
844 IKS infrared VEGA 1 measurements. In *ESLAB Symposium on the Exploration of Halley's Comet* (Vol. 250).

- 845 34. Engelhardt, T., Jedicke, R., Vereš, P., Fitzsimmons, A., Denneau, L., Beshore, E. and Meinke, B., 2017. An
846 observational upper limit on the interstellar number density of asteroids and comets. *The Astronomical*
847 *Journal*, 153:133, doi:10.3847/1538-3881/aa5c8a.
- 848 35. Farnham, T.L., Bodewits, D., Li, J.Y., Veverka, J., Thomas, P. and Belton, M.J.S., 2013. Connections between
849 the jet activity and surface features on Comet 9P/Tempel 1. *Icarus*, 222:540-549,
850 doi:10.1016/j.icarus.2012.06.019.
- 851 36. Feaga L.M., A'Hearn, M.F., Sunshine, J.M., Groussin, O. and Farnham, T.L., 2007. Asymmetries in the
852 distribution of H₂O and CO₂ in the inner coma of Comet 9P/Tempel 1 as observed by Deep Impact. *Icarus*,
853 191:134-145, doi:10.1016/j.icarus.2007.04.038.
- 854 37. Fernández, J.A., Tancredi, G., Rickman, H. and Licandro, J., 1999. The population, magnitudes, and sizes of
855 Jupiter family comets. *Astronomy and Astrophysics*, 352:327-340.
- 856 38. Flynn, G.J., 1990. The near-Earth enhancement of asteroidal over cometary dust. *Lunar and Planetary*
857 *Science Conference*, 20:363-371.
- 858 39. Flynn, G.J., 1994. Interplanetary dust particles collected from the stratosphere: Physical, chemical, and
859 mineralogical properties and implications for their sources. *Planetary and Space Science*, 42:1151-1161,
860 doi:10.1016/0032-0633(94)90014-0.
- 861 40. Flynn, G.J., Leroux, H., Tomeoka, K., Tomioka, N., Ohnishi, I., Mikouchi, T., Wirick, S., Keller, L.P., Jacobsen,
862 C. and Sanford, S.A., 2008. Carbonate in comets: a comparison of comets 1P/Halley, 9P/Tempel 1, and
863 81P/Wild 2. 39th Lunar and Planetary Science Conference; 10-14th March 2008, The Woodlands, TX; United
864 States (abstr.#1979).
- 865 41. Flynn, G.J., Wirick, S., Keller, L.P. and Jacobsen, C., 2009. STXM search for carbonate in samples of comet
866 81P/Wild 2. In *Journal of Physics: Conference Series* (Vol 186, No. 1, p. 012085). IOP Publishing,
867 doi:10.1088/1742-6596/186/1/012085.
- 868 42. Garrison, R.E., Luternauer, J.L., Grill, E.V., MacDonald, R.D. and Murray, J.W., 1969. Early diagenetic
869 cementation of recent sands, Fraser River delta, British Columbia. *Sedimentology*, 12:27-46,
870 doi:10.1111/j.1365-3091.1969.tb00162.x.
- 871 43. Gounelle, M., 2011. The asteroid–comet continuum: In search of lost primitivity. *Elements*, 7:29-34,
872 doi:10.2113/gselements.7.1.29.
- 873 44. Greenberg, J.M., Mizutani, H. and Yamamoto, T., 1995. A new derivation of the tensile strength of cometary
874 nuclei: application to comet Shoemaker-Levy 9. *Astronomy and Astrophysics*, 295:L35.
- 875 45. Groussin, O., A'Hearn, M.F., Li, J.Y., Thomas, P.C., Sunshine, J.M., Lisse, C.M., Meech, K.J., Farnham, T.L.,
876 Feaga, L.M. and Delamere, W.A., 2007. Surface temperature of the nucleus of Comet 9P/Tempel 1. *Icarus*,
877 187:16-25, doi:10.1016/j.icarus.2006.08.030.
- 878 46. Groussin, O., Sunshine, J.M., Feaga, L.M., Jorda, L., Thomas, P.C., Li, J.Y., A'Hearn, M.F., Belton, M.J.S., Besse,
879 S., Carcich, B. and Farnham, T.L., 2013. The temperature, thermal inertia, roughness and color of the nuclei
880 of Comets 103P/Hartley 2 and 9P/Tempel 1. *Icarus*, 222:580-594, doi:10.1016/j.icarus.2012.10.003.
- 881 47. Groussin, O., Jorda, L., Auger, A.T., Kührt, E., Gaskell, R., Capanna, C., Scholten, F., Preusker, F., Lamy, P.,
882 Hviid, S. and Knollenberg, J., 2015. Gravitational slopes, geomorphology, and material strengths of the
883 nucleus of comet 67P/Churyumov-Gerasimenko from OSIRIS observations. *Astronomy & Astrophysics*,
884 583:A32, doi:10.1051/0004-6361/201526379.
- 885 48. Guo, W. and Eiler, J.M., 2007. Temperatures of aqueous alteration and evidence for methane generation on
886 the parent bodies of the CM chondrites. *Geochimica et Cosmochimica Acta*, 71:5565-5575,
887 doi:10.1016/j.gca.2007.07.029.
- 888 49. Harker, D.E., Woodward, C.E. and Wooden, D.H., 2005. The dust grains from 9P/Tempel 1 before and after
889 the encounter with Deep Impact. *Science*, 310:278-280, doi:10.1126/science.1119143.
- 890 50. Harris, A.W. and Pravec, P., 2005. Rotational properties of asteroids, comets and TNOs. *Proceedings of the*
891 *International Astronomical Union*, 1:439-447, doi:10.1017/S1743921305006903.
- 892 51. Hartmann, W.K., Tholen, D.J. and Cruikshank, D.P., 1987. The relationship of active comets, "extinct"
893 comets, and dark asteroids. *Icarus*, 69:33-50, doi:10.1016/0019-1035(87)90005-4.

- 894 52. Hayward, T.L., Hanner, M.S. and Sekanina, Z., 2000. Thermal infrared imaging and spectroscopy of comet
895 Hale-Bopp (C/1995 O1). *The Astrophysical Journal*, 538, doi:10.1086/309117.
- 896 53. Hicks, L.J., MacArthur, J.L., Bridges, J.C., Price, M.C., Wickham-Eade, J.E., Burchell, M.J., Hansford, G.M.,
897 Butterworth, A.L., Gurman, S.J. and Baker, S.H., 2017. Magnetite in Comet Wild 2: Evidence for parent body
898 aqueous alteration. *Meteoritics & Planetary Science*, 52:2075-2096, doi:10.1111/maps.12909.
- 899 54. Hu, X., Gundlach, B., von Borstel, I., Blum, J. and Shi, X., 2019. Effect of radiative heat transfer in porous
900 comet nuclei: case study of 67P/Churyumov-Gerasimenko. *Astronomy & Astrophysics*, 630, doi:
901 10.1051/0004-6361/201834631.
- 902 55. Ishii, H.A., Bradley, J.P., Bechtel, H.A., Brownlee, D.E., Bustillo, K.C., Ciston, J., Cuzzi, J.N., Floss, C. and
903 Joswiak, D.J., 2018. Multiple generations of grain aggregation in different environments preceded solar
904 system body formation. *Proceedings of the National Academy of Sciences*, 115:6608-6613,
905 doi:10.1073/pnas.1720167115.
- 906 56. Jenniskens, P. and Jenniskens, P.M.M., 2006. Meteor showers and their parent comets. Cambridge
907 University Press.
- 908 57. Jenniskens, P., 2008. Meteoroid streams that trace to candidate dormant comets. *Icarus*, 194:13-22,
909 doi:10.1016/j.icarus.2007.09.016.
- 910 58. Jewitt, D. and Li, J., 2010. Activity in geminid parent (3200) Phaethon. *The Astronomical Journal*,
911 140:15191527, doi:10.1088/0004-6256/140/5/1519.
- 912 59. Joswiak, D.J., Brownlee, D.E., Matrajt, G., Westphal, A.J. and Snead, C.J., 2009. Kosmochloric Ca-rich
913 pyroxenes and FeO-rich olivines (Kool grains) and associated phases in Stardust tracks and chondritic porous
914 interplanetary dust particles: Possible precursors to FeO-rich type II chondrules in ordinary chondrites.
915 *Meteoritics & planetary science*, 44:1561-1588, doi:10.1111/j.1945-5100.2009.tb01192.x.
- 916 60. Keil, K., 2000. Thermal alteration of asteroids: evidence from meteorites. *Planetary and Space Science*,
917 48:887-903, doi:10.1016/S0032-0633(00)00054-4.
- 918 61. Keller, L.P. and Messenger, S., 2011. On the origins of GEMS grains. *Geochimica et Cosmochimica Acta*,
919 75:5336-5365, doi:10.1016/j.gca.2011.06.040.
- 920 62. Keller, H.U., Mottola, S., Hviid, S.F., Agarwal, J., Kührt, E., Skorov, Y., Otto, K., Vincent, J.B., Oklay, N.,
921 Schröder, S.E. and Davidsson, B., 2017. Seasonal mass transfer on the nucleus of comet 67P/Chuyumov-
922 Gerasimenko. *Monthly Notices of the Royal Astronomical Society*, 469:S357-S371,
923 doi:10.1093/mnras/stx1726.
- 924 63. Kelley, M.S. and Wooden, D.H., 2009. The composition of dust in Jupiter-family comets inferred from
925 infrared spectroscopy. *Planetary and Space Science*, 57:1133-1145, doi:10.1016/j.pss.2008.11.017.
- 926 64. Klöck, W., Thomas, K.L., McKay, D.S. and Palme, H., 1989. Unusual olivine and pyroxene composition in
927 interplanetary dust and unequilibrated ordinary chondrites. *Nature*, 339:126-128, doi:10.1038/339126a0.
- 928 65. Kokotanekova, R., Snodgrass, C., Lacerda, P., Green, S.F., Lowry, S.C., Fernández, Y.R., Tubiana, C.,
929 Fitzsimmons, A. and Hsieh, H.H., 2017. Rotation of cometary nuclei: new light curves and an update of the
930 ensemble properties of Jupiter-family comets. *Monthly Notices of the Royal Astronomical Society*, 471:2974-
931 3007, doi:10.1093/mnras/stx1716.
- 932 66. Kouchi, A., Greenberg, J.M., Yamamoto, T. and Mukai, T., 1992. Extremely low thermal conductivity of
933 amorphous ice-Relevance to comet evolution. *Astrophysical Journal*, 388:L73.
- 934 67. Królikowska, M. and Szutowicz, S., 2006. Non-gravitational motion of the Jupiter-family comet 81P/Wild 2-
935 I. The dynamical evolution. *Astronomy & Astrophysics*, 448:401-409, doi:10.1051/0004-6361:20053756.
- 936 68. Kömle, N.I. and Steiner, G., 1992. Temperature evolution of porous ice samples covered by a dust mantle.
937 *Icarus*, 96:204-212, doi:10.1016/0019-1035(92)90074-H.
- 938 69. Kömle, N.I., Steiner, G., Seidensticker, K.J., Kochan, H., Thomas, H., Thiel, K., Baguhl, M. and Höppner, B.,
939 1992. Temperature evolution and vapour pressure build-up in porous ices. *Planetary and space science*,
940 40:1311-1323, doi:10.1016/0032-0633(92)90088-6.
- 941 70. Kömle, N.I., Tiefenbacher, P., Weiss, P. and Bendiukova, A., 2018. Melting probes revisited—Ice penetration
942 experiments under Mars surface pressure conditions. *Icarus*, 308:117-127,
943 doi:10.1016/j.icarus.2017.08.006.

- 944 71. Lara, L.M., Lin, Z.Y., Rodrigo, R. and Ip, W.H., 2011. 67P/Churyumov-Gerasimenko activity evolution during
945 its last perihelion before the Rosetta encounter. *Astronomy & Astrophysics*, 525, doi:10.1051/0004-
946 6361/201015515.
- 947 72. Lee, M.R., Lindgren, P., Sofe, M.R., Alexander, C.O.D. and Wang, J., 2012. Extended chronologies of aqueous
948 alteration in the CM2 carbonaceous chondrites: Evidence from carbonates in Queen Alexandra Range
949 93005. *Geochimica et Cosmochimica Acta*, 92:148-169, doi:10.1016/j.gca.2012.06.005.
- 950 73. Licandro, J., Rubio, L.B., Casas, R., Gómez, A., Kidger, M.R., Sabalisk, N., Santos-Sanz, P., Serra-Ricart, M.,
951 Torres-Chico, R., Oscoz, A. and Jorda, L., 1997. The spin axis position of C/1995 O1 (Hale-Bopp). *Earth,*
952 *Moon, and Planets*, 77:199-206, doi:10.1023/A:1006291015391.
- 953 74. Lindgren, P., Hanna, R.D., Dobson, K.J., Tomkinson, T. and Lee, M.R., 2015. The paradox between low shock-
954 stage and evidence for compaction in CM carbonaceous chondrites explained by multiple low-intensity
955 impacts. *Geochimica et Cosmochimica Acta*, 148:159-178, doi:10.1016/j.gca.2014.09.014.
- 956 75. Lisse, C.M., Fernández, Y.R., Kundu, A., A'Hearn, M.F., Dayal, A., Deutsch, L.K., Fazio, G.G., Hora, J.L. and
957 Hoffmann, W.F., 1999. The nucleus of comet Hyakutake (C/1996 B2). *Icarus*, 140:189-204,
958 doi:10.1006/icar.1999.6131.
- 959 76. Lisse, C.M., A'hearn, M.F., Groussin, O., Fernández, Y.R., Belton, M.J.S., Van Cleve, J.E., Charmandaris, V.,
960 Meech, K.J. and McGleam, C., 2005. Rotationally resolved 8-35 micron Spitzer Space Telescope observations
961 of the nucleus of Comet 9P/Tempel 1. *The Astrophysical Journal Letters*, 625:L139, doi:10.1086/431238.
- 962 77. Lisse, C.M., VanCleve, J., Adams, A.C., A'hearn, M.F., Fernández, Y.R., Farnham, T.L., Armus, L., Grillmair, C.J.,
963 Ingalls, J., Belton, M.J.S. and Groussin, O., 2006. Spitzer spectral observations of the Deep Impact ejecta.
964 *Science*, 313:635-640, doi:10.1126/science.1124694.
- 965 78. Lisse, C.M., Kraemer, K.E., Nuth III, J.A., Li, A. and Joswiak, D., 2007. Comparison of the composition of the
966 Tempel 1 ejecta to the dust in Comet C/Hale-Bopp 1995 O1 and YSO HD 100546. *Icarus*, 191:223-240,
967 doi:10.1016/j.icarus.2006.11.027.
- 968 79. Love, S.G. and Brownlee, D.E., 1991. Heating and thermal transformation of micrometeoroids entering the
969 Earth's atmosphere. *Icarus*, 89:26-43, doi:10.1016/0019-1035(91)90085-8.
- 970 80. Mackinnon, I.D. and Rietmeijer, F.J., 1987. Mineralogy of chondritic interplanetary dust particles. *Reviews*
971 *of Geophysics*, 25:1527-1553, doi:10.1029/RG025i007p01527.
- 972 81. Madsen, B.G., 1997. Orbit determination and evolution of comet C/1995 O1 (Hale-Bopp). *Earth, Moon, and*
973 *Planets*, 79:3-15, doi:10.1023/A:1006268813208.
- 974 82. Maquet, L., 2015. The recent dynamical history of comet 67P/Churyumov-Gerasimenko. *Astronomy &*
975 *Astrophysics*, 579:A78, doi:10.1051/0004-6361/201425461.
- 976 83. McSween Jr, H.Y., Ghosh, A., Grimm, R.E., Wilson, L. and Young, E.D., 2002. Thermal evolution models of
977 asteroids. *Asteroids III*, 559.
- 978 84. Meech, K.J., Pittichová, J., Bar-Nun, A., Notesco, G., Laufer, D., Hainaut, O.R., Lowry, S.C., Yeomans, D.K. and
979 Pitts, M., 2009. Activity of comets at large heliocentric distances pre-perihelion. *Icarus*, 201:719-739,
980 doi:10.1016/j.icarus.2008.12.045.
- 981 85. Meech, K.J., Yang, B., Kleyana, J., Hainaut, O.R., Berdyugina, S., Keane, J.V., Micheli, M., Morbidelli, A. and
982 Wainscoat, R.J., 2016. Inner solar system material discovered in the Oort cloud. *Science Advances*,
983 2:e1600038, doi:10.1126/sciadv.1600038.
- 984 86. Miles, R., 2016. Heat of solution: A new source of thermal energy in the subsurface of cometary nuclei and
985 the gas-exsolution mechanism driving outbursts of Comet 29P/Schwassmann-Wachmann and other
986 comets. *Icarus*, 272:356-386, doi:10.1016/j.icarus.2015.12.053.
- 987 87. The Minor Planet Center 2019. Periodic comet orbit data accessible at:
988 <https://minorplanetcenter.net/iau/MPCORB/CometEls.txt>
- 989 88. Möhlmann, D., 2011. Three types of liquid water in icy surfaces of celestial bodies. *Planetary and Space*
990 *Science*, 59:1082-1086, doi:10.1016/j.pss.2010.09.005.
- 991 89. Mousis, O., Drouard, A., Vernazza, P., Lunine, J.I., Monnereau, M., Maggiolo, R., Altwegg, K., Balsiger, H.,
992 Berthelier, J.J., Cessateur, G. and De Keyser, J., 2017. Impact of radiogenic heating on the formation

- 993 conditions of comet 67P/Churyumov–Gerasimenko. *The Astrophysical journal letters*, 839:L4,
994 doi:10.3847/2041-8213/aa6839.
- 995 90. Mysen, E., 2004. Rotational dynamics of subsolar sublimating triaxial comets. *Planetary and Space Science*,
996 52:897-907, doi:10.1016/j.pss.2004.04.001.
- 997 91. Nakamura, K., Messenger, S. and Keller, L.P., 2005. TEM and NanoSIMS study of hydrated/anhydrous phase
998 mixed IDPs: cometary or asteroidal origin? 36th Lunar and Planetary Science Conference; 14-18th March
999 2005, The Woodlands, TX; United States (abstr.#1824).
- 1000 92. Nakamura-Messenger, K., Clemett, S.J., Messenger, S. and Keller, L.P., 2011. Experimental aqueous
1001 alteration of cometary dust. *Meteoritics & Planetary Science*, 46:843-856, doi:10.1111/j.1945-
1002 5100.2011.01197.x.
- 1003 93. Nelson, R., Nuth, J.A. and Donn, B., 1987. A kinetic study of the hydrous alteration of amorphous MgSiO
1004 smokes: Implications for cometary particles and chondrite matrix. *Journal of Geophysical Research: Solid*
1005 *Earth*, 92:657-662, doi:10.1029/JB092iB04p0E657.
- 1006 94. Nesvorný, D., Jenniskens, P., Levison, H.F., Bottke, W.F., Vokrouhlický, D. and Gounelle, M., 2010. Cometary
1007 origin of the zodiacal cloud and carbonaceous micrometeorites. Implications for hot debris disks. *The*
1008 *Astrophysical Journal*, 713:816-836, doi:10.1088/0004-637X/713/2/816.
- 1009 95. Noguchi, T., Nakamura, T., Okudaira, K., Yano, H., Sugita, S. and Burchell, M.J., 2007. Thermal alteration of
1010 hydrated minerals during hypervelocity capture to silica aerogel at the flyby speed of Stardust. *Meteoritics*
1011 *& Planetary Science*, 42:357-372, doi:10.1111/j.1945-5100.2007.tb00239.x.
- 1012 96. Noguchi, T., Ohashi, N., Tsujimoto, S., Mitsunari, T., Bradley, J.P., Nakamura, T., Toh, S., Stephan, T., Iwata,
1013 N. and Imae, N., 2015. Cometary dust in Antarctic ice and snow: Past and present chondritic porous
1014 micrometeorites preserved on the Earth's surface. *Earth and Planetary Science Letters*, 410:1-11,
1015 doi:10.1016/j.epsl.2014.11.012.
- 1016 97. Noguchi, T., Yabuta, H., Itoh, S., Sakamoto, N., Mitsunari, T., Okubo, A., Okazaki, R., Nakamura, T., Tachibana,
1017 S., Terada, K. and Ebihara, M., 2017. Variation of mineralogy and organic material during the early stages of
1018 aqueous activity recorded in Antarctic micrometeorites. *Geochimica et Cosmochimica Acta*, 208:119-144,
1019 doi:10.1016/j.gca.2017.03.034.
- 1020 98. Nuth, J.A., Abreu, N.M., Clark, B., Johnson, N.M. and Glavin, D.P., 2019. Do We Need a New Definition for a
1021 Comet? 82nd Annual Meeting of The Meteoritical Society, (Abstr. #2452).
- 1022 99. Ohtsuka, K., Nakato, A., Nakamura, T., Kinoshita, D., Ito, T., Yoshikawa, M. and Hasegawa, S., 2009. Solar-
1023 radiation heating effects on 3200 Phaethon. *Publications of the Astronomical Society of Japan*, 61:1375-
1024 1387, doi:10.1093/pasj/61.6.1375.
- 1025 100. Pajola, M., Höfner, S., Vincent, J.B., Ockay, N., Scholten, F., Preusker, F., Mottola, S., Naletto, G., Fornasier,
1026 S., Lowry, S. and Feller, C., 2017. The pristine interior of comet 67P revealed by the combined Aswan
1027 outburst and cliff collapse. *Nature Astronomy*, 1:1-8, doi:10.1038/s41550-017-0092.
- 1028 101. Pätzold, M., Andert, T.P., Hahn, M., Barriot, J.P., Asmar, S.W., Häusler, B., Bird, M.K., Tellmann, S.,
1029 Oschlisniok, J. and Peter, K., 2019. The Nucleus of comet 67P/Churyumov–Gerasimenko—Part I: The global
1030 view—nucleus mass, mass-loss, porosity, and implications. *Monthly Notices of the Royal Astronomical*
1031 *Society*, 483:2337-2346, doi:10.1093/mnras/sty3171.
- 1032 102. Podolak, M. and Prialnik, D., 1997. 26 Al and liquid water environments in comets. In *Comets and the Origin*
1033 *and Evolution of Life*. 259-272. Springer, New York, NY.
- 1034 103. Prialnik, D. and Bar-Nun, A., 1990. Gas release in comet nuclei. *The Astrophysical Journal*, 363:274-282.
- 1035 104. Prialnik, D. and Bar-Nun, A., 1992. Crystallization of amorphous ice as the cause of comet P/Halley's outburst
1036 at 14 AU. *Astronomy and astrophysics*, 258:L9-L12.
- 1037 105. Prialnik, D., Bar-Nun, A., and Podolak, M., 1987. Radiogenic heating of comets by Al-26 and implications for
1038 their time of formation. *The Astrophysical Journal*, 319:993-1002.
- 1039 106. Quirico, E., Moroz, L.V., Beck, P., Schmitt, B., Arnold, G., Bonal, L. and RV Team, 2015. Composition of comet
1040 67P/Churyumov-Gerasimenko refractory crust as inferred from VIRTIS-M/ROSETTA spectro-imager.
1041 Proceedings European Planetary Science Congress (EPSC, Abstr.#2092).

- 1042 107.Reach, W.T., Vaubaillon, J., Lisse, C.M., Holloway, M. and Rho, J., 2010. Explosion of comet 17P/Holmes as
1043 revealed by the Spitzer space telescope. *Icarus*, 208:276-292, doi:10.1016/j.icarus.2010.01.020.
- 1044 108.Rhim, J.W., 2011. Effect of clay contents on mechanical and water vapour barrier properties of agar-based
1045 nanocomposite films. *Carbohydrate polymers*, 86:691-699, doi:10.1016/j.carbpol.2011.05.010.
- 1046 109.Richardson, J.E., Melosh, H.J., Lisse, C.M. and Carcich, B., 2007. A ballistics analysis of the Deep Impact ejecta
1047 plume: Determining Comet Tempel 1's gravity, mass, and density. *Icarus*, 191:176-209,
1048 doi:10.1016/j.icarus.2007.08.033.
- 1049 110.Rietmeijer, F.J., 1985. A model for diagenesis in proto-planetary bodies. *Nature*, 313:293-294,
1050 doi:10.1038/313293a0.
- 1051 111.Rietmeijer, F.J., 1991. Aqueous alteration in five chondritic porous interplanetary dust particles. *Earth and
1052 Planetary Science Letters*, 102:148-157, doi:10.1016/0012-821X(91)90004-2.
- 1053 112.Rietmeijer, F.J., Nuth III, J.A. and Nelson, R.N., 2004. Laboratory hydration of condensed magnesiosilica
1054 smokes with implications for hydrated silicates in IDPs and comets. *Meteoritics & Planetary Science*, 39:723-
1055 746, doi:10.1111/j.1945-5100.2004.tb00115.x.
- 1056 113.Rubin, A.E., 2012. Collisional facilitation of aqueous alteration of CM and CV carbonaceous chondrites.
1057 *Geochimica et Cosmochimica Acta*, 90:181-194, doi:10.1016/j.gca.2012.05.016.
- 1058 114.Russo, N.D., Mumma, M.J., DiSanti, M.A., Magee-Sauer, K., Novak, R. and Rettig, T.W., 2000. Water
1059 production and release in Comet C/1995 O1 Hale-Bopp. *Icarus*, 143:324-337, doi:10.1006/icar.1999.6268.
- 1060 115.Sanzovo, G.C., De Almeida, A.A., Misra, A., Torres, R.M., Boice, D.C. and Huebner, W.F., 2001. Mass-loss
1061 rates, dust particle sizes, nuclear active areas and minimum nuclear radii of target comets for missions
1062 STARDUST and CONTOURP. *Monthly Notices of the Royal Astronomical Society*, 326:852-868,
1063 doi:10.1046/j.1365-8711.2001.04443.x.
- 1064 116.Schultz, P.H., Hermalyn, B. and Veverka, J., 2013. The deep impact crater on 9P/Tempel-1 from Stardust-
1065 NExT. *Icarus*, 222:502-515, doi:10.1016/j.icarus.2012.06.018.
- 1066 117.Schulz, R., Hilchenbach, M., Langevin, Y., Kissel, J., Silen, J., Briois, C., Engrand, C., Hornung, K., Baklouti, D.,
1067 Bardyn, A. and Cottin, H., 2015. Comet 67P/Churyumov-Gerasimenko sheds dust coat accumulated over the
1068 past four years. *Nature*, 518, doi:10.1038/nature14159.
- 1069 118.Sekanina, Z., 1988. Outgassing asymmetry of periodic comet Encke. I-Apparitions 1924-1984. *The
1070 Astronomical Journal*, 95:911-924.
- 1071 119.Sekanina, Z., 2002. Statistical investigation and modeling of sungrazing comets discovered with the Solar
1072 and Heliospheric Observatory. *The Astrophysical Journal*, 566:577-598, doi:10.1086/324335.
- 1073 120.Shi, X., Hu, X., Sierks, H., Güttler, C., A'hearn, M., Blum, J., El-Maarry, M.R., Kührt, E., Mottola, S., Pajola, M.
1074 and Ockay, N., 2016. Sunset jets observed on comet 67P/Churyumov-Gerasimenko sustained by subsurface
1075 thermal lag. *Astronomy & Astrophysics*, 586, doi:10.1051/0004-6361/201527123.
- 1076 121.Sierks, H., Barbieri, C., Lamy, P.L., Rodrigo, R., Koschny, D., Rickman, H., Keller, H.U., Agarwal, J., A'hearn,
1077 M.F., Angrilli, F. and Auger, A.T., 2015. On the nucleus structure and activity of comet 67P/Churyumov-
1078 Gerasimenko. *Science*, 347, doi:10.1126/science.aaa1044.Steckloff, J.K., Johnson, B.C., Bowling, T., Melosh,
1079 H.J., Minton, D., Lisse, C.M. and Battams, K., 2015. Dynamic sublimation pressure and the catastrophic
1080 breakup of Comet ISON. *Icarus*, 258:430-437, doi:10.1016/j.icarus.2015.06.032.
- 1081 122.Snodgrass, C., Opitom, C., de Val-Borro, M., Jehin, E., Manfroid, J., Lister, T., Marchant, J., Jones, G.H.,
1082 Fitzsimmons, A., Steele, I.A. and Smith, R.J., 2016. The perihelion activity of comet 67P/Churyumov-
1083 Gerasimenko as seen by robotic telescopes. *Monthly Notices of the Royal Astronomical Society*, 462:S138-
1084 S145, doi:10.1093/mnras/stw2300.
- 1085 123.Soderblom, L.A., Britt, D.T., Brown, R.H., Buratti, B.J., Kirk, R.L., Owen, T.C. and Yelle, R.V., 2004. Short-
1086 wavelength infrared (1.3–2.6 μm) observations of the nucleus of Comet 19P/Borrelly. *Icarus*, 167:100-112,
1087 doi:10.1016/j.icarus.2003.08.019
- 1088 124.Spohn, T., Knollenberg, J., Ball, A.J., Banaszkiewicz, M., Benkhoff, J., Grott, M., Grygorczuk, J., Hüttig, C.,
1089 Hagermann, A., Kargl, G. and Kaufmann, E., 2015. Thermal and mechanical properties of the near-surface
1090 layers of comet 67P/Churyumov-Gerasimenko. *Science*, 349, doi:10.1126/science.aab0464.

- 1091 125.Starkey, N.A., Franchi, I.A. and Lee, M.R., 2014. Isotopic diversity in interplanetary dust particles and
1092 preservation of extreme 16O-depletion. *Geochimica et Cosmochimica Acta*, 142:115-131,
1093 doi:10.1016/j.gca.2014.07.011.
- 1094 126.Stodolna, J., Gainsforth, Z., Butterworth, A.L. and Westphal, A.J., 2014. Characterization of preserved
1095 primitive fine-grained material from the Jupiter family comet 81P/Wild 2—A new link between comets and
1096 CP-IDPs. *Earth and Planetary Science Letters*, 388:367-373, doi:10.1016/j.epsl.2013.12.018.
- 1097 127.Takigawa, A., Furukawa, Y., Kimura, Y., Davidsson, B. and Nakamura, T., 2019. Exposure Experiments of
1098 Amorphous Silicates and Organics to Cometary Ice and Vapour Analogs. *The Astrophysical Journal*, 881:27,
1099 doi:10.3847/1538-4357/ab27c6.
- 1100 128.Thomas, N., Alexander, C. and Keller, H.U., 2008. Loss of the surface layers of comet nuclei. *Space science*
1101 *reviews*, 138:165-177, doi:10.1007/s11214-008-9332-5.
- 1102 129.Trigo-Rodriguez, J.M. and Blum, J., 2009. Tensile strength as an indicator of the degree of primitiveness of
1103 undifferentiated bodies. *Planetary and Space Science*, 57:243-249, doi:10.1016/j.pss.2008.02.011.
- 1104 130.Tosi, F., Capaccioni, F., Capria, M.T., Mottola, S., Zinzi, A., Ciarniello, M., Filacchione, G., Hofstadter, M.,
1105 Fonti, S., Formisano, M. and Kappel, D., 2019. The changing temperature of the nucleus of comet 67P
1106 induced by morphological and seasonal effects. *Nature Astronomy*, 453:649-658 doi:10.1038/s41550-019-
1107 0740-0.
- 1108 131.Vacher, L.G., Marrocchi, Y., Villeneuve, J., Verdier-Paoletti, M.J. and Gounelle, M., 2018. Collisional and
1109 alteration history of the CM parent body. *Geochimica et Cosmochimica Acta*, 239:213-234,
1110 doi:10.1016/j.gca.2018.08.006.
- 1111 132.Vacher, L.G., Piralla, M., Gounelle, M., Bizzarro, M. and Marrocchi, Y., 2019. Thermal Evolution of Hydrated
1112 Asteroids Inferred from Oxygen Isotopes. *The Astrophysical Journal Letters*, 882:L20, doi:10.3847/2041-
1113 8213/ab3bd0/meta.
- 1114 133.Vaubailon, J. and Colas, F., 2005. Demonstration of gaps due to Jupiter in meteoroid streams. What
1115 happened with the 2003 Pi-Puppids? *Astronomy & Astrophysics*, 431:1139-1144, doi:10.1051/0004-
1116 6361:20041391.
- 1117 134.Verdier-Paoletti, M.J., Marrocchi, Y., Avice, G., Roskosz, M., Gurenko, A. and Gounelle, M., 2017. Oxygen
1118 isotope constraints on the alteration temperatures of CM chondrites. *Earth and Planetary Science Letters*,
1119 458:273-281, doi:10.1016/j.epsl.2016.10.055.
- 1120 135.Walsh, K.J., Morbidelli, A., Raymond, S.N., O'Brien, D.P. and Mandell, A.M., 2012. Populating the asteroid
1121 belt from two parent source regions due to the migration of giant planets—“The Grand Tack”. *Meteoritics*
1122 *& Planetary Science*, 47:1941-1947, doi:10.1111/j.1945-5100.2012.01418.x.
- 1123 136.Weaver H.A., Mumma M.J., Larson H.P. 1988. Infrared investigation of water in comet P/Halley. In: Grewing
1124 M., Praderie F., Reinhard R. (eds) *Exploration of Halley's Comet*. Springer, Berlin, Heidelberg, 411-418,
1125 doi:10.1007/978-3-642-82971-0_75
- 1126 137.Whipple, F.L. and Sekanina, Z., 1979. Comet Encke—Precession of the spin axis, nongravitational motion, and
1127 sublimation. *The Astronomical Journal*, 84:894-1909.
- 1128 138.Wickramasinghe, J.T., Wickramasinghe, N.C. and Wallis, M.K., 2009. Liquid water and organics in Comets:
1129 implications for exobiology. *International Journal of Astrobiology*, 8:281-290,
1130 doi:10.1017/S1473550409990127.
- 1131 139.Wooden, D.H., Harker, D.E., Woodward, C.E., Butner, H.M., Koike, C., Witteborn, F.C. and McMurtry, C.W.,
1132 1999. Silicate mineralogy of the dust in the inner coma of comet C/1995 01 (Hale-Bopp) pre-and
1133 postperihelion. *The Astrophysical Journal*, 517, doi:10.1086/307206.
- 1134 140.Wozniakiewicz, P.J., Ishii, H.A., Kearsley, A.T., Burchell, M.J., Bradley, J.P., Teslich, N. and Cole, M.J., 2010.
1135 Survivability of cometary phyllosilicates in Stardust collections and implications for the nature of comets.
1136 41st Lunar and Planetary Science Conference; 1-5 Mar. 2010; The Woodlands, TX; United States
1137 (abstr.#2357).
- 1138 141.Yabuta, H., Noguchi, T., Itoh, S., Nakamura, T., Miyake, A., Tsujimoto, S., Ohashi, N., Sakamoto, N.,
1139 Hashiguchi, M., Abe, K.I. and Okubo, A., 2017. Formation of an ultracarbonaceous Antarctic micrometeorite

1140 through minimal aqueous alteration in a small porous icy body. *Geochimica et Cosmochimica Acta*, 214:172-
1141 190, doi:10.1016/j.gca.2017.06.047.

1142 142.Yeomans, D.K., Giorgini, J.D. and Chesley, S.R., 2005. The history and dynamics of Comet 9P/Tempel 1. *Space*
1143 *Science Reviews*, 117:123-135, doi:10.1007/s11214-005-3392-6

1144 143.Younger, J.P., Reid, I.M., Vincent, R.A. and Murphy, D.J., 2012. Meteor shower velocity estimates from
1145 single-station meteor radar: accuracy and precision. *Monthly Notices of the Royal Astronomical Society*,
1146 425:1473-1478, doi:10.1111/j.1365-2966.2012.21632.x.

1147 144.Zolensky, M.E., Zega, T.J., Yano, H., Wirick, S., Westphal, A.J., Weisberg, M.K., Weber, I., Warren, J.L., Velbel,
1148 M.A., and 66 other authors. 2006. Mineralogy and petrology of comet 81P/Wild 2 nucleus samples. *Science*,
1149 314:1735-1739, doi:10.1126/science.1135842.

1150 145.Zolensky, M., Nakamura-Messenger, K., Rietmeijer, F., Leroux, H., Mikouchi, T., Ohsumi, K., Simon, S.,
1151 Grossman, L., Stephan, T., Weisberg, M. and Velbel, M., 2008. Comparing Wild 2 particles to chondrites and
1152 IDPs. *Meteoritics & Planetary Science*, 43:261-272, doi:10.1111/j.1945-5100.2008.tb00621.x.

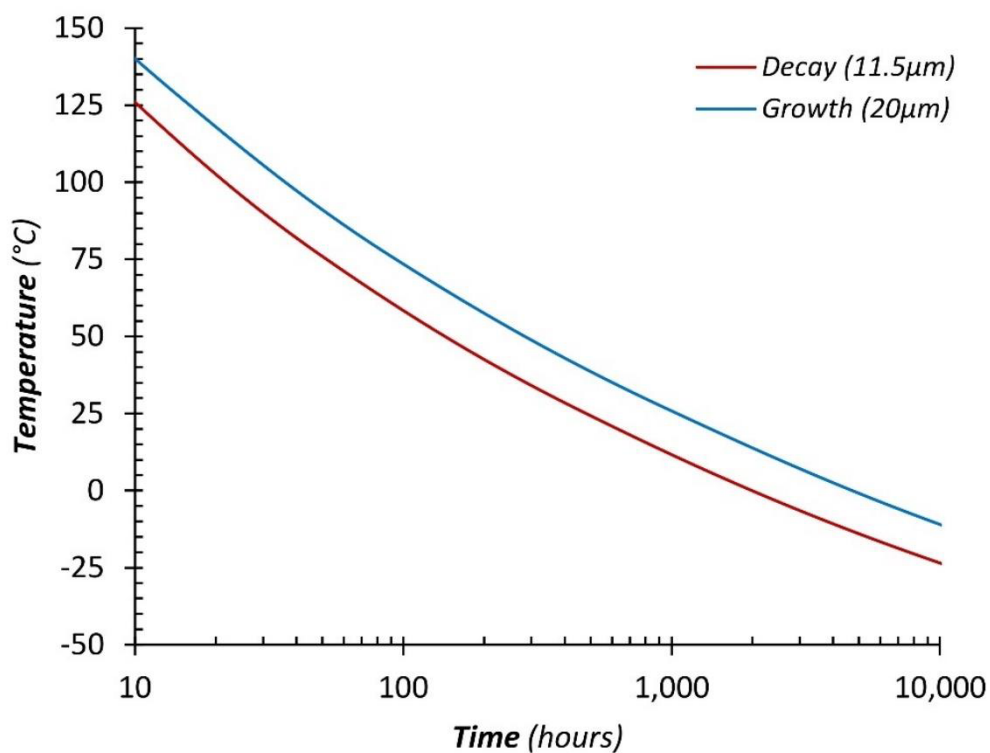
1153

1154 **11. List of figures and tables**

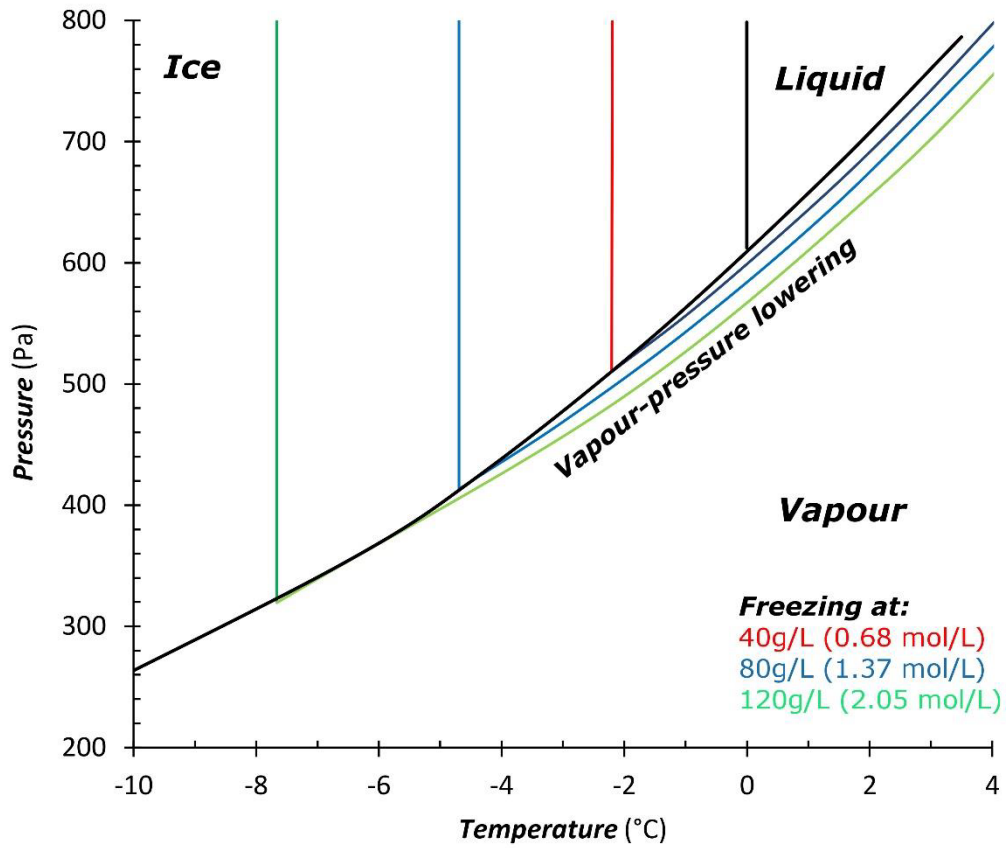
- 1155 **Fig.1.** Experimentally determined aqueous alteration reaction rate dependence on temperature
1156 **Fig.2** Pressure-temperature phase diagram for water-ice showing freezing point depression for saline solutions
1157 **Fig.3.** Spacecraft measured comet surface temperatures from IR instruments
1158 **Fig.4.** Predicted shallow depth internal temperatures for 5 spacecraft-visited comets
1159 **Fig.5.** Rotational periods for 37 Jupiter Family comets
1160 **Fig.6.** Pressure-temperature phase diagram for water-ice, with cometary subsurface temperatures and
1161 pressure estimates added.
1162 **Fig.7.** Alteration timescales, how long does the subsurface have to alter before being eroded?
1163 **Fig.8.** Comet orbit data showing perihelion distances of periodic comets

1164

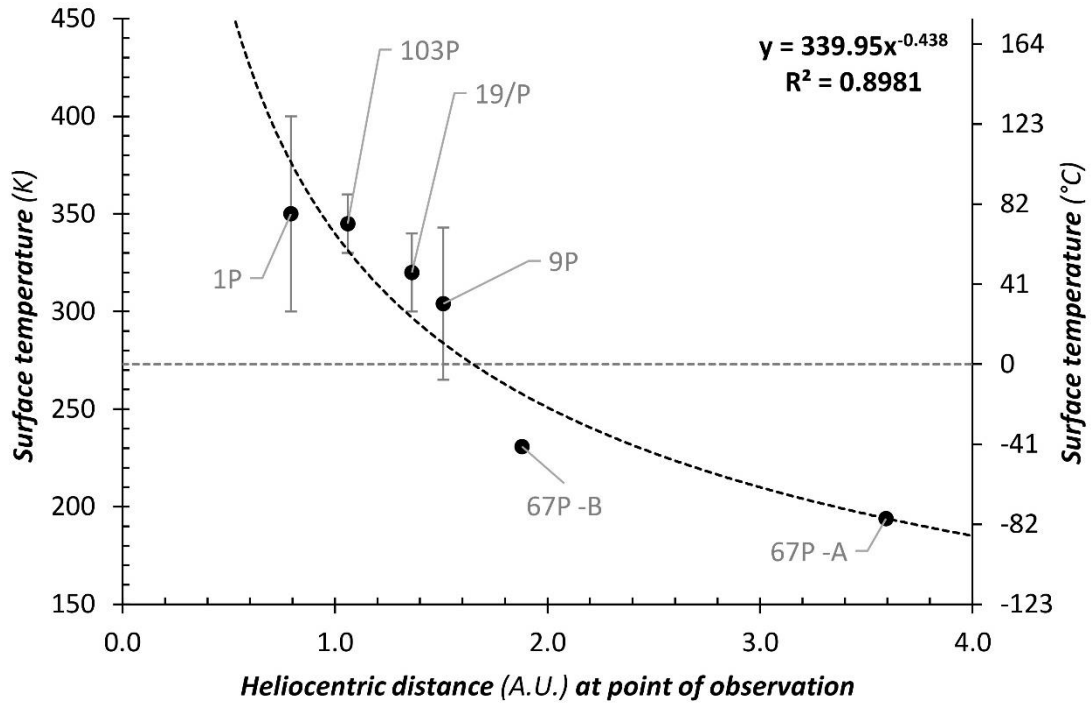
1165 **Fig.1.** Reaction rate kinetics relevant to the aqueous alteration of GEMS within a cometary subsurface. This plot
1166 displays an empirically determined temperature-dependence relationship for the hydration of amorphous Mg-
1167 SiO “smokes”. The measured reaction products are sepiolite (a complex partial chain phyllosilicate). Data were
1168 taken from Nelson et al., (1987). However, we note that the absolute reaction times needed for the hydration
1169 of naturally-occurring GEMS to form primitive phyllosilicates (serpentine/saponite) are likely to be significantly
1170 shorter than the reaction times displayed here – perhaps two orders of magnitude shorter, as demonstrated by
1171 the alteration of anhydrous GEMS in Nakamura et al., (2011). Despite this duration discrepancy the temperature
1172 dependence relationship is likely accurate. The red and blue lines reflect the decay and growth of different
1173 spectral features as measured by IR spectroscopy.
1174



1175 **Fig.2.** Water-ice phase diagram illustrating the action of increasing salinity (higher concentration NaCl solutions
1176 [red lowest concentration, green highest concentration]) on freezing point depression. Impure water has a
1177 significantly lower temperature and vapour pressure than pure water. Cometary water is unlikely to be pure,
1178 but instead mixed with a range of salts, potentially NaCl as well as sulfate salts. (Data from [Feistel et al., 2008](#)).
1179
1180

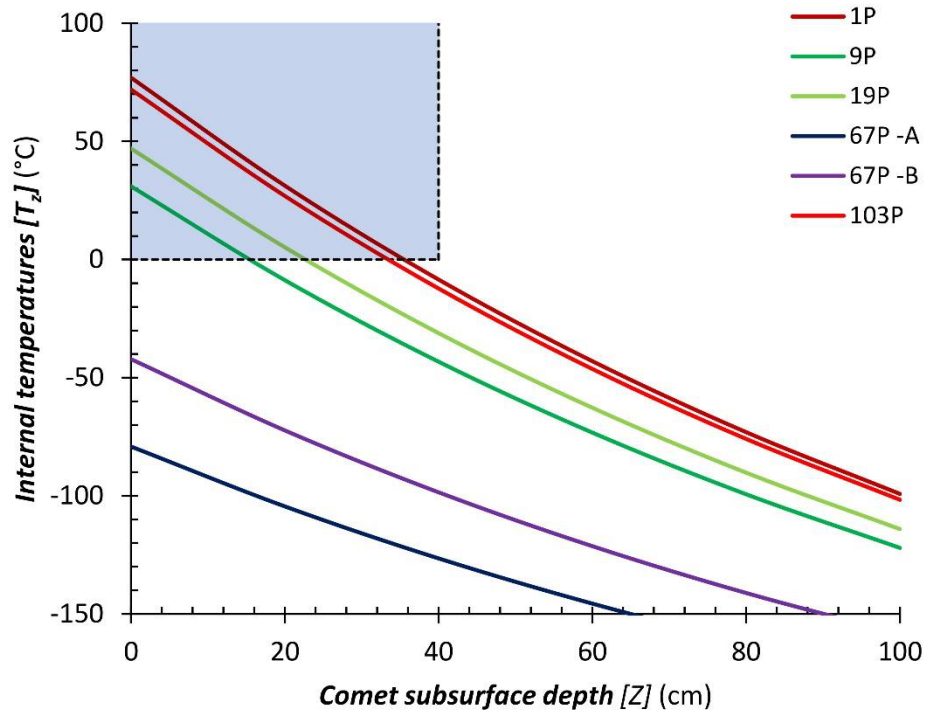


1181 **Fig.3.** Measured comet surface temperature vs. heliocentric distance for five periodic comets (1P, 9P, 19P, 67P
 1182 and 103P). Data derived from: Emerich, et al., (1986), Soderblom et al., (2004), Groussin et al., (2007; 2013) and
 1183 Tosi et al., (2019). Black points mark their average surface temperature while grey error bars reflect the level of
 1184 variation at the surface. For 67P we include two independent measurements points "A" and "B" as referred to
 1185 in Tosi et al., (2019) and measured at different heliocentric distances.
 1186

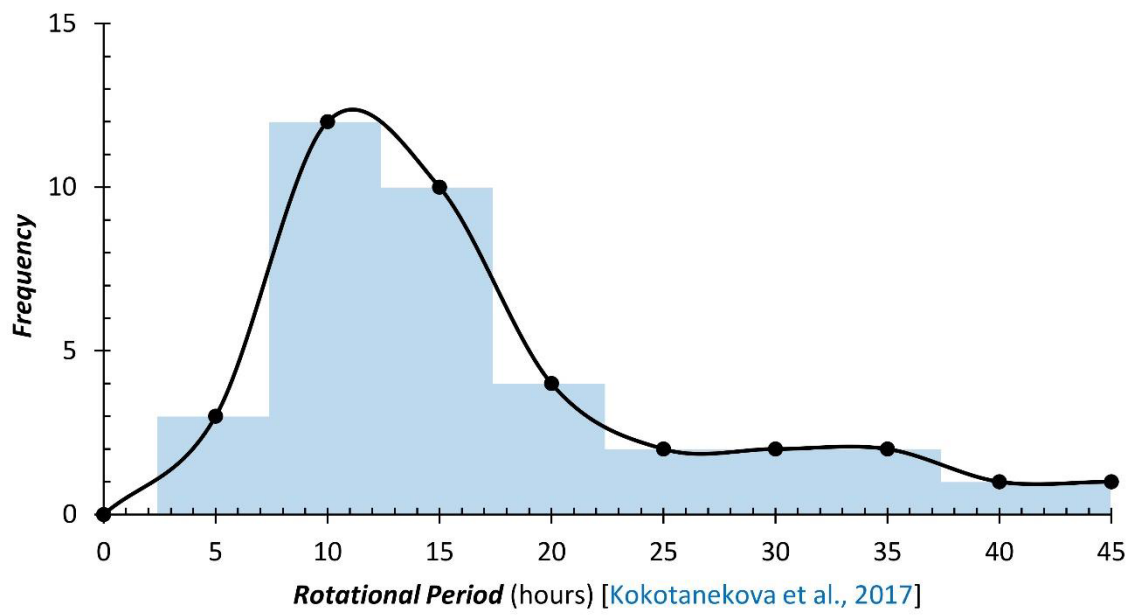


1187

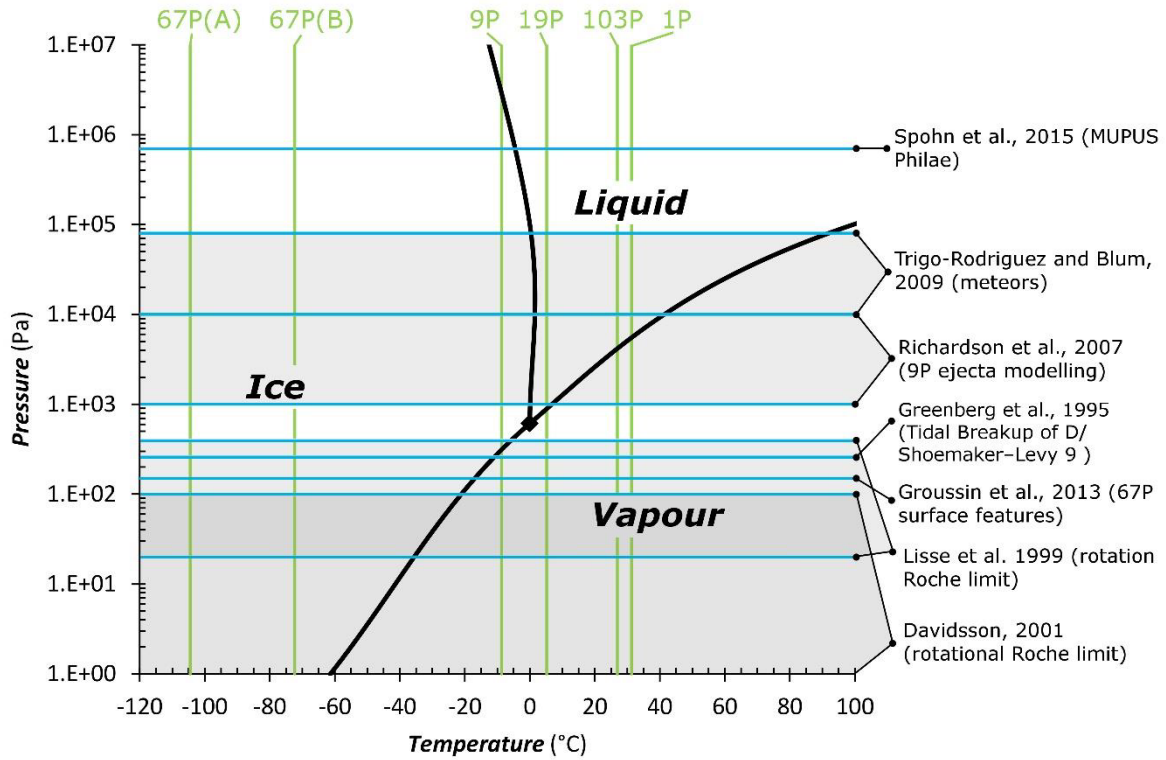
1188 **Fig.4.** Internal comet subsurface temperatures at perihelion for five periodic comets (1P, 9P, 19P, 67P and 103P),
1189 inferred from measured surface temperatures (spacecraft data) and the thermal conduction model of
1190 Wickramasinghe et al., (2009). We mark the region at which liquid water may be viable as a shaded blue box,
1191 showing that temperatures $>0^{\circ}\text{C}$ could exist down to depths of 40cm on some periodic comets (including 1P, 9P,
1192 19P and 103P).
1193
1194



1195 **Fig.5.** Rotational periods for 37 Jupiter Family comets, varying between 2.8 and 41 hours with a mean average
1196 value of 14.4 hours and a median average value of 10.9 hours. Data taken from Kokotanekova et al., (2017).
1197

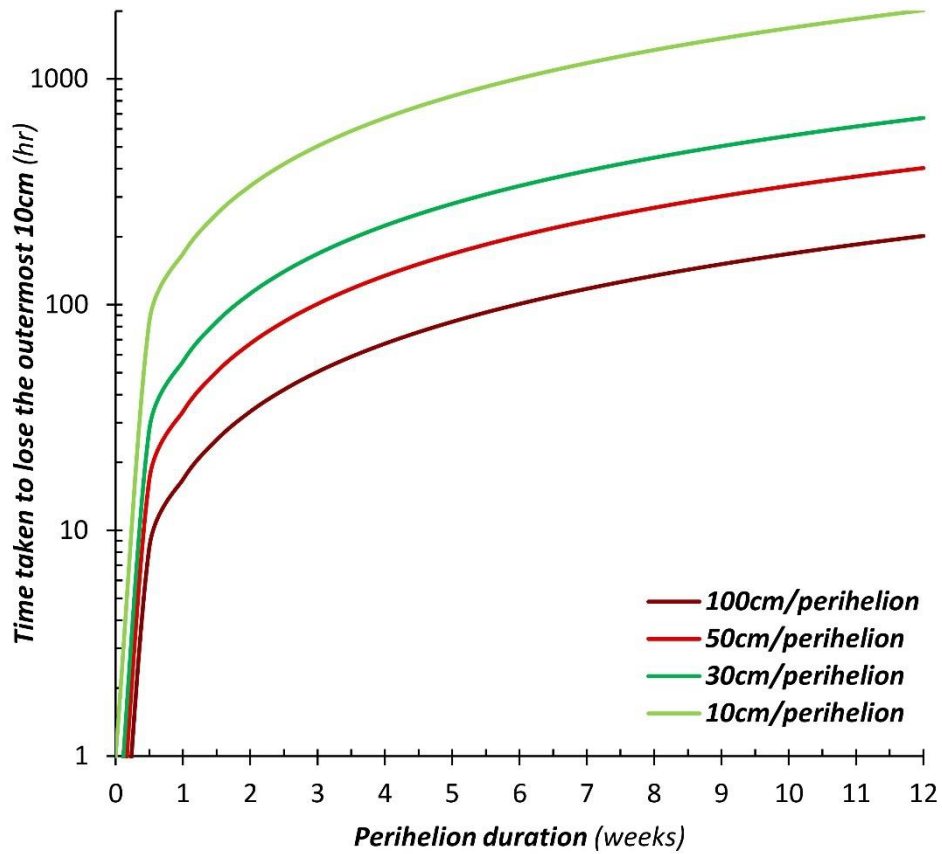


1198 **Fig.6.** The pressure-temperature phase diagram of pure water-ice showing the stability field for liquid water.
 1199 Impurities will shift the liquid stability field to lower temperatures (Fig. 2), making liquid water more stable on
 1200 9P/Tempel 1. Green lines show the predicted internal temperature (at shallow depths [20cm]) for 5 periodic
 1201 comets whose surface temperatures have been constrained by spacecraft data. Blue lines plot tensile strength
 1202 estimates for comets based on spacecraft, meteoroid and modelling data (<270Pa, [Greenberg et al., 1995](#); 20-
 1203 400Pa, [Lisse et al. 1999](#); <100Pa, [Davidsson, 2001](#); 150Pa [Groussin et al., 2013](#); 1-10kPa, [Richardson et al.](#)
 1204 [2007](#); 10-80kPa, [Trigo-Rodriguez and Blum, 2009](#) and 700kPa from [Spohn et al., 2015](#)).
 1205

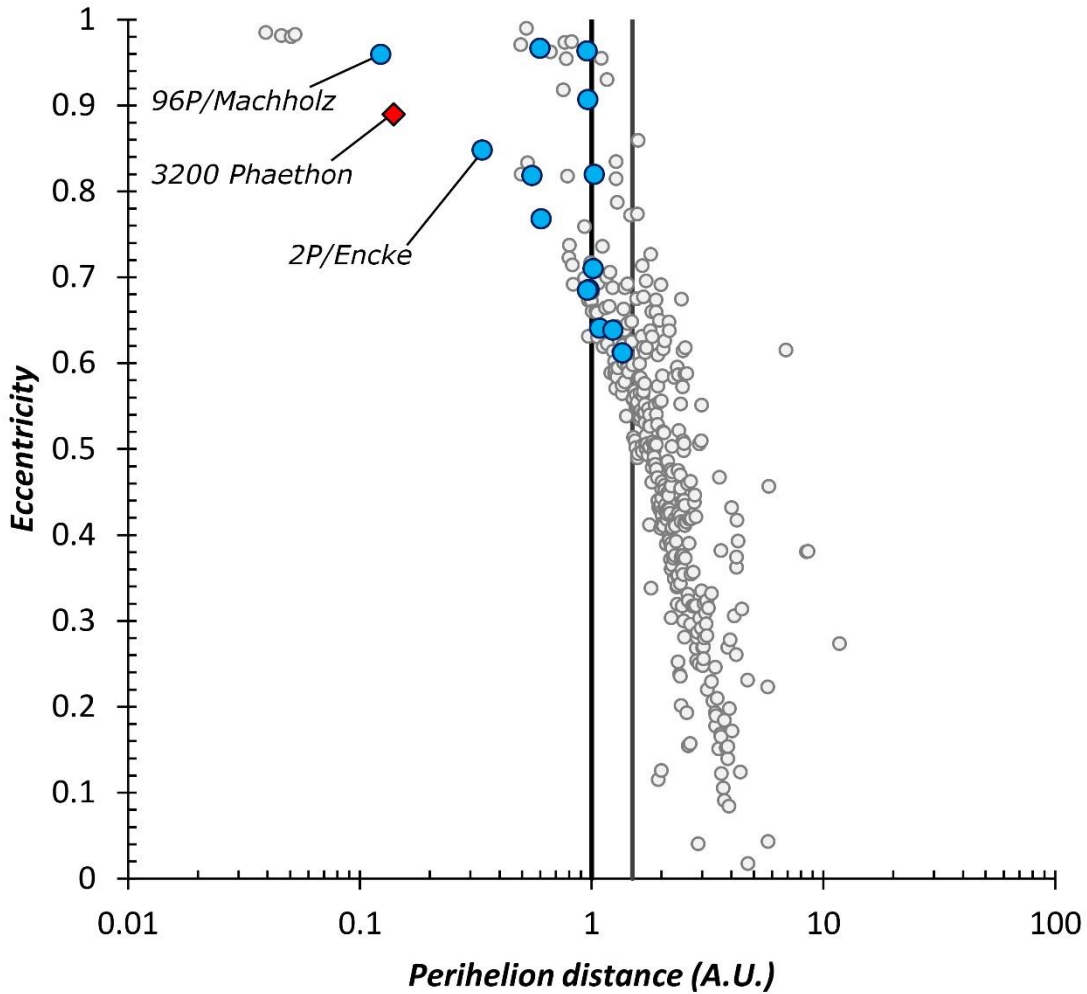


1206
 1207
 1208
 1209

1210 **Fig.7.** Comparing alteration timescales. This plot shows how long the outermost 10cm of a comet nucleus will
1211 survive during a perihelion pass, dependent on the total amount of material shed (between 10-100cm, based
1212 on existing literature estimates) and the duration over which this mass loss occurs. The duration over which the
1213 outer surface is shed is poorly constrained but appears to be <12 weeks (2016 hours).
1214
1215



1216 **Fig.8.** Orbit data (perihelion distance [in A.U.] vs. eccentricity) for 367 known periodic comets. Data taken from
1217 the Minor Planet Center (2019). Black and grey bold lines mark perihelion distances of 1.0 and 1.5 A.U.
1218 respectively. Ninety-one comets (24.8% of the total) have orbits <1.5 A.U., while 35 comets (9.5% of the total)
1219 have orbits <1.0 A.U. Those which pass closest to the Sun during perihelion are most likely to support subsurface
1220 liquid water. Blue circles denote comets associated with an active meteor shower reaching Earth today, as
1221 described in Jenniskens and Jenniskens (2006) and Jenniskens (2008). The red diamond shows the orbital data
1222 for the active asteroid 3200 Phaethon, associated with the late December Geminids meteor shower. Also
1223 labelled are 2P/Encke and 96P/Machholz. Note: this plot also shows how small bodies orbits are affected by tidal
1224 circularization, reducing their eccentricity.
1225



1226
1227
1228
1229
1230
1231